

8-3-2020

Evaluation of Engineered Thermal Refuge in Streams as a Climate Warming Mitigation Strategy for Fish Populations Experiencing Thermal Stress

Rebekah Thielman
rebekah.thielman@uconn.edu

Follow this and additional works at: https://opencommons.uconn.edu/gs_theses

Recommended Citation

Thielman, Rebekah, "Evaluation of Engineered Thermal Refuge in Streams as a Climate Warming Mitigation Strategy for Fish Populations Experiencing Thermal Stress" (2020). *Master's Theses*. 1531.
https://opencommons.uconn.edu/gs_theses/1531

This work is brought to you for free and open access by the University of Connecticut Graduate School at OpenCommons@UConn. It has been accepted for inclusion in Master's Theses by an authorized administrator of OpenCommons@UConn. For more information, please contact opencommons@uconn.edu.

Evaluation of Engineered Thermal Refuge in Streams as a Climate Warming Mitigation Strategy for Fish Populations Experiencing Thermal Stress

Rebekah Thielman

B.S., Wheaton College, 2018

A Thesis

Submitted in Partial Fulfillment of the

Requirements for the Degree of

Master of Science

At the

University of Connecticut

2020

APPROVAL PAGE

Masters of Science Thesis

**Evaluation of Engineered Thermal Refuge in
Streams as a Climate Warming Mitigation
Strategy for Fish Populations Experiencing
Thermal Stress**

Presented by

Rebekah Thielman, B.S.

Major

Advisor _____

Amvrossios C. Bagtzoglou

Co-Major Advisor

Advisor _____

Martin A. Briggs

Associate

Advisor _____

Jason Vokoun

University of Connecticut

2020

ACKNOWLEDGEMENTS

First, I would like to thank my co-major advisor Dr. Martin A. Briggs for all the support and guidance he has given me over the course of this research these two years. I sincerely appreciate all his work in keeping me directed toward my goals, and providing constant help and assistance along the way. I am also very grateful for the encouragement and input of Dr. Amvrossios Bagtzoglou in supporting me in my research and course work, and providing insightful feedback on my work. I'd also like to thank Dr. Jason Vokoun for all of his field work expertise and helpful insight on my project and presentations, and providing natural resources expertise. I greatly appreciate the opportunity to work with all three of these committee members.

I also am grateful for the Helton lab group, for their continual input on all things professional development and research related, and for encouraging me in my goals and completing this thesis. I also would like to thank Amvrossios Bagtzoglou's research group for their support, their interesting research updates, and helping me become a better researcher.

I'd like to thank the Environmental Engineering Department faculty and staff for their support in all of my course work endeavors, and the USGS geophysics branch for all the amazing opportunities they provided and equipment know-how and fieldwork help. I'd like to thank Megan Upp and Maggie Chafouleas for all of their field work assistance and hard work in helping me in my research.

Last, I would like to thank my family for supporting me during this time, encouraging me, and listening to me talk about my research, and Sprocket my cat for all her undivided attention and input.

Table of Contents

ACKNOWLEDGEMENTS	III
ABSTRACT	V
INTRODUCTION	1
1.1 BACKGROUND	1
1.2 GOALS AND OBJECTIVES.....	4
METHODS.....	5
2.1 FIELD SITE.....	5
2.2 GROUNDWATER INJECTION	8
2.4 VELOCITY FLOW CHARACTERIZATION	16
RESULTS.....	17
3.1 FIELD SITE BATHYMETRY AND TOPOGRAPHY	17
3.2 COLD WATER DISCHARGE	20
DISCUSSION.....	43
CONCLUSIONS.....	51
APPENDIX	52
WORKS CITED	61

ABSTRACT

Rising summer stream temperatures threaten the habitat of cold-water fishes globally. Streams with cold groundwater seeps can provide thermal refuge, however natural groundwater discharge is often patchy throughout watersheds, impacting habitat connectivity. This research was undertaken to evaluate the potential to engineer (active pumping) thermal refuge that mimic cold groundwater seeps under a range of natural streamflow conditions and varying cold-water injection rates. Natural groundwater averaging 10 °C was pumped into the river channel behind a removable baffle, used to inhibit mixing and dispersal of the groundwater plume. A fiber-optic distributed temperature sensing cable was deployed above the streambed, downstream of the injection point. Visible light and thermal infrared images were collected of the water surface. The goal of this research was to collect data at high, medium, and low natural stream discharges in the Fenton River near the University of Connecticut in Storrs, CT, USA, as well as test high, medium, and low injection rates relative to typical monitoring well pump rates. The range of cold anomalies monitored by the FO-DTS cable indicated a -0.09 °C temperature drop between the surface water and minimum temperature in the cold-water plume at high flow stream discharge, -0.31°C temperature change for medium discharge, and a -1.1°C temperature decrease for low stream flow discharge. The three varied rate pumping tests indicated that an increase in pumping rate creates a slightly cooler plume, but does not make a substantially large difference at an overall stream discharge rate of 0.42 m³/s at the Fenton River.

INTRODUCTION

1.1 Background

Stream ecology is heavily influenced by thermal regimes: water temperature directly impacts the development of aquatic organisms, species distribution, microbial metabolic rates, along with their ecosystem processes and services (Kløve et al. 2014). Cold-water adapted aquatic organisms have evolved to be dependent on groundwater discharge in streams as a protective buffer against variable annual temperatures (Ebersole et al. 2003). While thermal 'refugia' are typically thought of as larger-scale cold water habitat, thermal 'refuge' are discrete meter-scale colder-water patches created by groundwater seepage, emergent hyporheic exchange, tributary confluence, or riparian shading, and are often found in discontinuous zones within the stream reach (Kurylyk et al. 2015). As air temperatures rise and short duration droughts increase due to anticipated climate change (Isaak et al. 2015, Huntington et al. 2009), cold-water species will need to rely more heavily on natural thermal refuge to survive, especially during periods where peak temperatures exceed their metabolic threshold. However, natural thermal refuges are often not well distributed along stream corridors (Petty et al. 2012), may not be well protected from aerial predation, and their effectiveness may decrease as shallow groundwater also warms (Briggs et al. 2018a).

Cold-water adapted fish species are highly adept at seeking out cooler temperatures within their habitat and using these areas to thermoregulate (Hitt et al. 2016). Behavioral thermoregulation is a strategy used by fish to maintain their thermal threshold by seeking out ideal temperature ranges within their thermally heterogeneous

habitat, whether in a stratified lake, or a stream with heterogeneous pockets of cold and warm water (Peterson et al. 1996). Fish in a lake in Wisconsin containing effluent from a power plant were distributed by size and temperature preferences around and in the effluent plume (Neill et al. 1974). This stratification did not change regardless of increased food sources outside of their selected areas. Studies performed on salmon and trout with thermal tracking found them able to maintain body temperatures significantly lower than that of the main stream reach which had reached temperatures greater than their survival threshold (Baird and Krueger, 2003, Mathews and Berg, 1997), by congregating in areas with groundwater seeps or springs, suggesting that their survival in areas with high surface temperatures is dependent on their access to cold-water discharges (Petty et al. 2012, Snook et al. 2016). Trout and other cold-water adapted fish species have been observed to create microhabitats within their watershed based on groundwater discharge zones and separate out their habitats based on species size and their ideal temperature range (Torgersen et al. 2012). Additionally, studies of salmon indicate that the fish alter their migration activity in pursuit of spawning grounds and in order to behaviorally thermoregulate in cool tributaries while surface waters remain at peak and stressful temperatures (Gonia et al. 2006).

In marginal thermal habitat, cold-water fish behavioral strategies rely on natural thermal refuge, which sources range from groundwater seeps and springs, deeper hyporheic exchange, riparian shading or deep points within the stream bathymetry, and tributary confluence (Kurylyk et al. 2015). While these mechanisms can potentially be utilized by cold-water adapted species for thermoregulation, it is difficult for some species to access them due to the uneven distribution of groundwater seeps and tributaries

throughout watersheds, resulting in species isolation and fragmentation. Many natural cold-water pockets may be exposed to aerial predators, particularly stream confluence zones, and are therefore not suitable to serve as refuge (Peterson et al. 1996, Briggs et al. 2018b). Also, due to human alterations to streams, riparian shading and hyporheic exchange may become disrupted, further limiting natural thermal refuge and decreasing cold thermal input (Gonia et al. 2006). Groundwater flowing shallowly beneath the surface (up to ~5 m) is also at risk to temperature fluctuations and warming trends (Kurylyk et al. 2014, Briggs et al. 2018c). In addition to the limited availability of natural refuge, feeding opportunities can become sparse for cold-water adapted species in the few crowded, cool areas available (Baird and Krueger, 2003). Migrating species experience higher pre-spawn mortality in areas with too much exposure to high surface temperatures (Gonia et al. 2006). Mortality related to diseases is also heightened under increased temperatures, as microorganisms experience increased growth, combined with fish species' lowered immunity due to their experienced thermal stress (Crozier et al. 2014). These factors put fish species at risk as they face warmer temperatures and less refuge available to them to alleviate thermal stress.

Due to inherent challenges presented by natural thermal refuge, human 'engineered' cold water pockets may be a viable addition to help cold-water species survive hot periods (Kurylyk et al. 2015). In general, physical stream restoration projects are seeking to better incorporate ecological services and are focusing on altering thermal regimes through riparian cover, hyporheic exchange remediation (Doll et al. 2003, Hare et al. 2017), and augmenting natural thermal refuge with artificial refuge, by mimicking groundwater seeps (Kurylyk et al. 2015). In the summer season when cold-water adapted

species are faced with peak temperatures for short periods of time, a cold-water refuge created by pumping nearby aquifer groundwater directly into the stream reach could provide protection from lethal temperatures. While these pumped point-scale inputs may not serve to lower the overall temperature of the surface water, it would create a thermal refuge by creating a spatially focused cold pocket under the ‘right’ hydrodynamic conditions (Kurylyk et al. 2015; Briggs and Hare, 2018).

1.2 Goals and Objectives

The primary goal of this research was to assess the effectiveness of actively pumped groundwater thermal refuge as a climate-change adaption strategy for cold-water adapted species that live in streams at risk for lethal temperatures during the summer months. In order to do this, nearby alluvial aquifer groundwater was pumped into a wide section of the Fenton River, CT at controlled rates during peak temperature periods of the summer season by using an existing riparian well. For the variable pump rate tests, a water tank was used containing enough ice to create the same temperature as natural groundwater. The extent of the cold thermal anomaly created was assessed using a combination of temperature sensing methods, while mixing was assessed with visual dye and hydrodynamic measurement methods. The objectives of this study were to

- 1) Characterize effective cold-water plume footprint created by pumping groundwater across a natural gradient of in channel flow rates.
- 2) Determine the effect of varying typical groundwater pump rates on the extent of cold-water plume produced in the surface water.
- 3) Assess the effectiveness of an engineered baffle at limiting local mixing of

surface water with groundwater, and testing the effect of varying cold-water injection methods on the dispersion of the cold-water plume.

METHODS

2.1 Field Site

The study area is point along the Fenton River located in Tolland County, CT which is part of the Natchaug River Watershed and is an overall gaining stream, covering a drainage area of 18.3 mi². (Warner et al. 2006). The upstream USGS stream gage 01121330 provides the field site with a sub-daily record of river discharge and gage height every 15 minutes. The time of year initially chosen for the three experiments at variable stream discharges (August, 2018) was chosen based on the mean discharge over the past 7 years as recorded by the USGS Fenton River gage, which showed March to be the peak flow month of the year with 1.9 m³/s, July to be the driest with 0.3 m³/s, and the medium flow rate of 1.0 m³/s in May. Streams in Connecticut lie on the margin between cold and warm water habitat, with temperature gradients that often result in both cold and warm water adapted species spatially distributed based on temperature. The Fenton river provides a site that is cool enough to contain cold-water adapted species but will be among the highest risk riverine systems to experience exceedance of species' thermal thresholds due to climate change. It also provides proximity to the University of Connecticut's monitoring and production well field, allowing easy access to shallow, alluvial aquifer groundwater for pumping for an engineered thermal refuge. The stream is home to a number of different species, including native Brook trout, both important recreationally and ecologically; Brook trout are known to be an indicator species of clean,

cold groundwater (Warner et al. 2006, Kanno et al. 2013). Brook and Brown trout have also been observed to decrease in growth when temperatures exceed 16 °C, and their estimated upper thermal threshold hovers around 23 to 24 °C (Chadwick et al. 2017), causing much of the Fenton River to become a hazardous habitat for several days each summer. The Fenton study reach also contains natural cold groundwater seeps, as depicted below using thermal infrared imaging. These cold groundwater seeps exemplify the type of natural thermal buffer an engineered refuge would augment, as we were not able to document any substantial natural cold-water plumes emanating from natural seeps along this Fenton River reach.

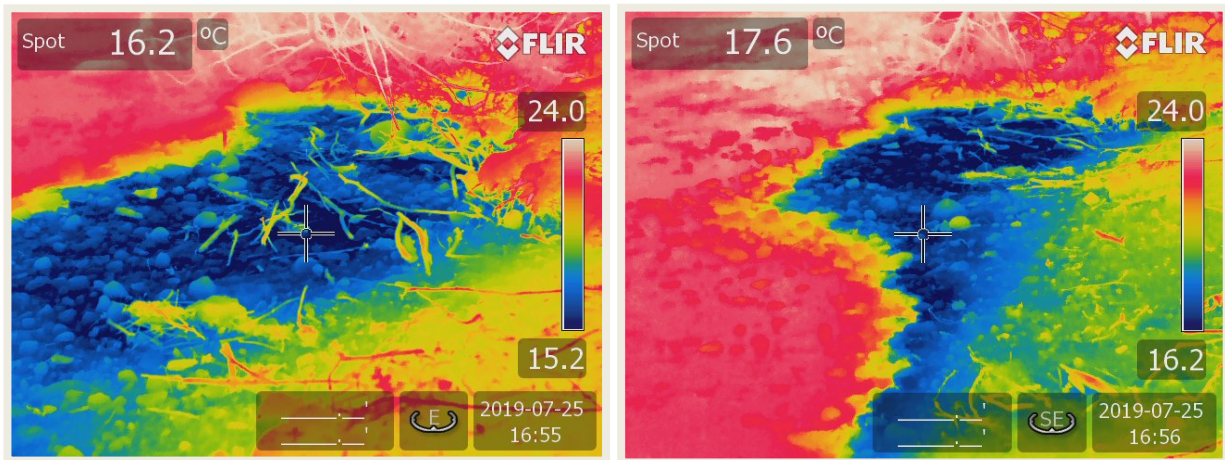


Figure 1. Infrared images of cold, natural seep found approximately 1-km downstream of the field site along the Fenton river emanating from a sand and gravel bank.

The location for the injection site of groundwater and subsequent temperature monitoring equipment setup within the river was selected due to its nearness to well MW 4S-99 (Figure 2), to minimize the distance required to pump the groundwater, and the well's ability to pump at a sustained high flow rate, producing clear, minimally turbid

flow. A series of well tests were performed on wells in the area within the ideal distance to the Fenton, and the well and field site were selected based on these tests.

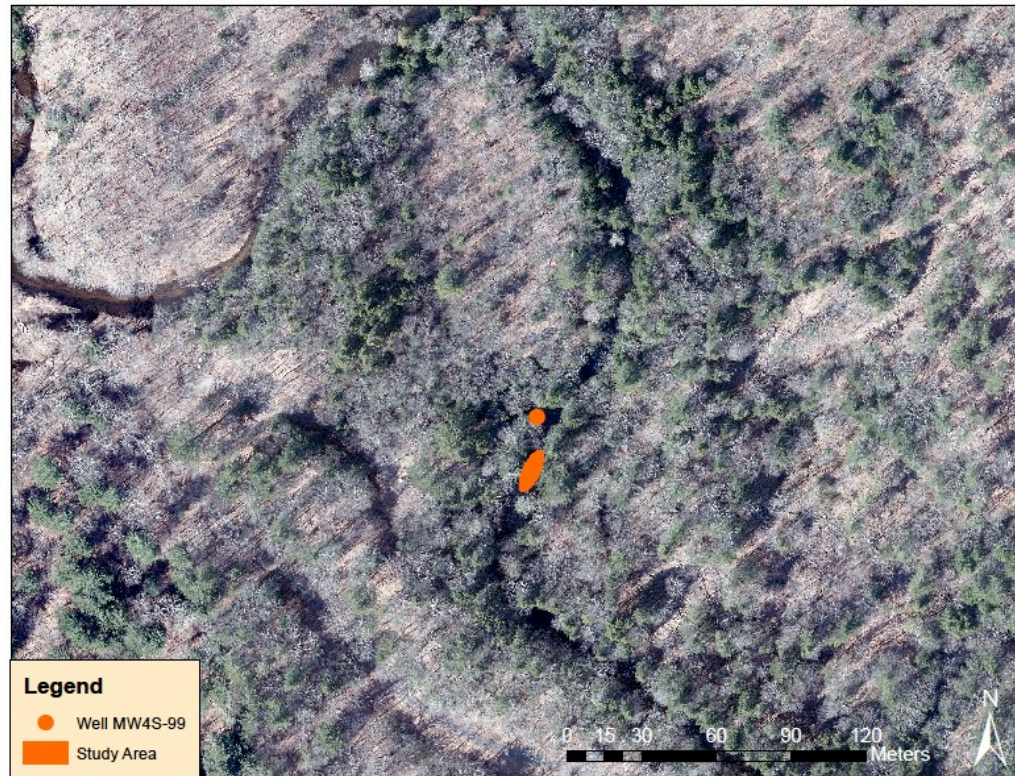


Figure 2. Aerial overview of field site in the Fenton River.

The location of the baffle and injection point of the groundwater within the stream channel was selected in the middle of the stream reach instead of along the banks due to the location's relative depth in order to prevent the spot from drying up during base flow conditions. It was also selected due to its riparian shading in order to maximize sunlight for images of the dye tracer in the surface water.

In order to characterize the field site, the bathymetry of the streambed field site and the surrounding topography were surveyed using a total station (Nikon Nivo) for both years in which experiments were performed, 2018 and 2019. This also included spatial characterization of the baffle, rebar, pump hose line, well, well house, and other

identifiable landmarks. A total of 436 points were taken to characterize the area, with 342 points in 2018, and 94 points in 2019.

2.2 Groundwater injection

Before pumping groundwater to the stream reach, the well (MW4S-99) was assessed for its ability to be pumped at a sustained, consistent rate, and also its ability to produce minimally turbid water at a relatively cooler temperature than the surface water (Vokoun et al. 2016). After a series of well tests, the water was determined to be a mean of 10 °C in the well (approximately the annual surface temperature mean), and 11-12 °C after being pumped through the hose line to the discharge point in the stream reach which was 13 meters away. Its depth to water was 2.1 meters and recharge rate was 32 seconds after filling 37.9 liters, with a 30.5 cm outer diameter casing and 6.55 meter screen length. The pump used in conjunction with the well was a submersible Grundfos MP 1/ Rediflo 2 pump capable of pumping at a maximum rate of 26.5 L/min at 400 Hz. It was selected due to its accessibility as a commonly used pump for household well water extraction, and its ability to pump at a maximum rate for up to 500 hours and at precise rates. It required a 3.3 kVA (2.64 kW) generator to run. A realized rate pump test was performed using a 37.9 liter bucket with six trials, averaging a rate of 0.41 L/s. Well water was pumped through 15.2 meters of reinforced PVC braided tubing with a 2.54 cm inner diameter and flowed through a distributed release slotted pipe placed on the streambed to mimic a natural groundwater seep. Large stakes held up the hosing connecting the pump to the discharge location to prevent it from trailing in the water and warming prematurely to entering the discharge pipe, and the discharge pipe was placed

directly behind the baffle in the area where stream flow was assumed to be lowest due to the disruption of the channel flow path created by the obstruction. The baffle was created with four 1 meter long untreated wooden boards cut to a uniform size and stacked two on top of each other vertically. They were held in place by metal rings screwed into the wood, which attached to rebar staked into the streambed in order to hold the boards in a V-shape. The v-shaped obstruction pointed upstream and was designed to disrupt the channel flow and prevent the surface water from mixing immediately with the groundwater due to the groundwater being pumped to a discrete point instead of seeping in a uniform front like in natural thermal refuge (Kurylyk et al. 2015). The slotted release pipe was placed directly behind the point of this v-shaped baffle, and was made from a PVC pipe with a capped end, with slots drilled into the sides for the groundwater to seep out of.



Figure 3. Image of groundwater discharge setup, with hose line, baffle, and FO-DTS measurement system (blue cable).

In addition to pumping at a consistent rate (0.41 L/s) across a range of stream discharges in the Fenton River, on a low flow discharge day (0.4 m³/s), variable pumping rates were tested using a sump pump and stock tank to deliver cold-water instead of pumping from the well. This was done on a low flow discharge day (July 25, 2019) in order to maximize the presence of the cold-water plume. As the Grundfos pump was broken during earlier experiments, a submersible Dai Bao sump pump with a variable rate controller was used. These variable rate experiments required a 750 L stock tank filled with water from the stream reach that was subsequently cooled with ice to approximate groundwater temperature (~10 °C), as the sump pump is not designed for

groundwater extraction (does not fit down the well). The sump pump was connected to a standard garden hose line (1.6 cm diameter), and used to pump stream water into the tank. A NIST-certified Traceable 4000 digital thermometer was used to determine the surface water temperature at 22.94 °C. In order to mimic the cold groundwater pumped previously from the well at 10 °C, approximately 110 kg of ice were added to the stock tank to drop the temperature down from 22.94 °C to 10 °C. An aquarium bubbler was used to keep the tank mixed and to ensure even temperature distribution throughout the tank as the ice melted. Once at the desired temperature, the sump pump was connected to the hose line and the slotted distributed release pipe was used again as the cold-water injection method, and placed directly behind the baffle in the same area of the stream reach as used previously. This allowed for three pump tests to be performed at 11 L/min, 19 L/min, and 23 L/min while maintaining the same temperature sensing methods. Additionally, at the medium pump rate, 19 L/min, temperature data was collected for a different groundwater injection technique: instead of allowing the groundwater to flow through the slotted distributed release uncovered as before, the pipe was covered with cobbles and substrate in order to further mimic a buried groundwater seep.

200 Hz		250 Hz		300 Hz	
Trial	Rate (L/min)	Trial	Rate (L/min)	Trial	Rate (L/min)
1	11.58	1	14.82	1	17.88
2	11.52	2	14.88	2	18.24
3	11.82	3	14.82	3	18.06
MEAN:	11.64		14.84		18.06
350 Hz		375 Hz		400 Hz	
Trial	Rate (L/min)	Trial	Rate (L/min)	Trial	Rate (L/min)
1	22.20	1	22.62	1	23.40
2	20.52	2	22.92	2	22.56
3	20.58	3	22.92	3	23.28
MEAN:	21.1		22.82		23.08

Table 1. Realized rate pumping tests in L/min performed in the Fenton River using a Grundfos Rediflo pump.

The first two well-pumping experiments performed were on a high river flow day ($1.8 \text{ m}^3/\text{s}$) after a rainfall event and a medium flow day ($1.0 \text{ m}^3/\text{s}$) on August 15 and 16, 2018 respectively. Due to an unusually wet summer and fall low baseflow conditions were not achieved in 2018 at the Fenton, and the low river flow experiment ($0.4 \text{ m}^3/\text{s}$) was performed on July 2, 2019.

Next, on another day of low flow discharge (July 15, 2019), the three pump tests were performed at 11 L/min, 19 L/min, and 23 L/min, in order to test different injection rates and depict the resulting plumes. At 19 L/min (medium variable pumping rate), different groundwater injection methods were tested by comparing the resulting plumes created after burying the slotted distributed release pipe under cobbles and substrate, versus leaving it placed on the streambed uncovered. The resulting cold-water plumes were compared.

Pump test 1		Pump Test 2		Pump 3	
Time (s)	Rate (L/min)	Time (s)	Rate (L/min)	Time (s)	Rate (L/min)
99	11.47	100	11.36	103	11.02
91	12.48	104	10.92	105	10.81
91	12.48	108	10.52	90	12.61
Mean:	12.14	Mean:	10.93	Mean:	11.48
Pump 4		Pump Test 5			
Time (s)	Rate (L/min)	Time (s)	Rate (L/min)		
59	19.25	48.33	23.51		
60	18.93	50.72	22.37		
60	18.93	50.89	22.71		
		51.9	21.88		
Mean:	19.04	Mean:	22.62		

Table 2. Realized rate pumping tests in L/s performed in the Fenton River using a sump pump.

2.3 Thermal Imaging

To assess the extent of the cold groundwater plume created through the pump-injection setup, three different imaging technologies were used to detect the movement of the colder groundwater (9-11°C) in the surface water (19 °C - 23°C).

- 1) Thermal infrared images were used to distinguish any thermal anomalies at the surface (i.e. Handcock et al. 2012).
- 2) A FO-DTS system was used to detect cold-water plumes created along the streambed interface (i.e. Rosenberry et al. 2016, Briggs et al. 2012).
- 3) Brilliant Blue Dye injected into the pump line was used as a tracer to visualize where the groundwater was moving within the water column and how rapidly it was mixing with the surface water. Natural light photos were taken of this progression.

After the pump had run till the injection rate was stabilized, a FLIR T-640 infrared camera with stated accuracy of $\pm 2^{\circ}\text{C}$ and 640 x 480 resolution was used to image the surface of the stream reach around the baffle and downstream of the baffle from the groundwater injection site. Images were taken from the top of a ladder positioned directly above the baffle in order to minimize reflection from incoming solar radiation. The imaging was used to detect thermal anomalies at the water surface on all three variable discharge days (1.8 m³/s, 1.0 m³/s, and 0.4 m³/s), and for the three variable rate pump

tests (11.4 L/min, 18.9 L/min, and 22.7 L/min). Remote sensing of emitted thermal radiation is an efficient method to detect the spatial distribution of surface heat in rivers, but it only captures the ‘skin’ surface layer of the water, nothing deeper than the top 100 μm .

To detect thermal anomalies beneath the surface of the water column, a FO-DTS cable was positioned approximately 11 cm above the streambed (on average), and wrapped around 0.2 m diameter metal pulley wheels held in place by 0.6 m rebar stake inserted into the streambed. The cable was wrapped around the pulleys in order to prevent bending or kinking of the fiber optic glass within the cable at the turn points. This setup created a crisscross grid downstream behind the baffle, as depicted in Figure 4 using 213 meters of the cable and covering an area of 48 m^2 . The cable was laid upstream of the baffle in order to characterize the water temperature outside the area of cold-water injection. The middle, left, and right-side portions of the cable wrapped around the pulley wheels which were attached to the rebar were spatially identified using the Nikon Nivo total station by marking where the cable was located at the apex of the turn on the pulley wheel on the left and right hand sets of rebar, and the spatial location of the middle of the cable between each pulley. This spatial survey data informed the spatial distribution of temperature through time collected by the FO-DTS cable by interpolating between known cable positions using USGS DTSGUI software (Domanski et al., 2019). The configuration was used for all six experiments, in the same position of the stream reach each day. It detected temperature through time at 0.25 m resolution along the cable.

The third component of qualitatively evaluating the spatial extent of the cold-water plume involved using a 4 g/L mix of Brilliant Blue tracer dye, injected with a

syringe into the hose line delivering the groundwater from the well into the stream reach (Figure 4). For the variable rate pump tests, the dye was added to the tank and allowed to mix evenly before photographing using an aquarium bubbler to thoroughly distribute the dye throughout. After each injection, a progression of photos was taken depicting the dispersion of the groundwater downstream after exiting the slotted release pipe. These natural light photos were typically taken from the stream bank in order to capture the full area with baffle and FO-DTS array downstream. 17 photos were taken on the 1.8 m³/s flow day, 21 on the 1.0 m³/s flow day, and 8 on the 0.4 m³/s flow day. 47 photos total were taken for the variable pump rate tests, and an approximation of the extent of the plume was made using these photos and the total station spatial data.



Figure 4. Brilliant blue dye injected into the groundwater hose line using a syringe and released into the stream water column downstream of the baffle.

2.4 Velocity Flow Characterization

To assess how effective the baffle was at disrupting flow and preventing the surface water from immediately mixing with the cooler groundwater, the flow-field of the stream site was measured in multiple planes using a Flowtracker Handheld-ADV in conjunction with the Nikon Nivo total station. Velocity in m/s, direction (from upstream) in degrees, and depth in meters were calculated using the Flowtracker at points within the fiber-optic grid downstream of the baffle, in addition to points taken around and in front of the baffle structure. At each point at which the velocity was determined, the total station spatially identified the location of each data point collected. The flow field was also characterized without the baffle on the medium flow day ($1.0 \text{ m}^3/\text{s}$), in order to create a comparison between the effect of the upstream structure on creating a slower flowing pocket within the stream reach. This flow field assessment was also used on the low flow and high flow days ($0.4 \text{ m}^3/\text{s}$ and $1.8 \text{ m}^3/\text{s}$). 99 velocity points were taken total, with 24 on the $1.8 \text{ m}^3/\text{s}$ flow day, 56 on the $1.0 \text{ m}^3/\text{s}$ flow day, and 19 points on the $0.4 \text{ m}^3/\text{s}$ flow day.

Another way in which the effectiveness of the baffle at delaying surface water from mixing with the groundwater was determined was through pumping the cold-water into the stream reach with and without the baffle present, and allowing the fiber optic cable to collect temperature data downstream over time for both scenarios. This comparison data was collected on the medium discharge day, at $1.0 \text{ m}^3/\text{s}$, and allowed for the two cold water plumes to be compared with and without the baffle.

RESULTS

3.1 Field Site Bathymetry and Topography

The spatial data collected from the Nikon Nivo total station characterizing the study area bathymetry and topography for both years in which experiments were performed (2018, 2019) were created using a spline interpolation of the measured positions in ArcMap, and the elevation.

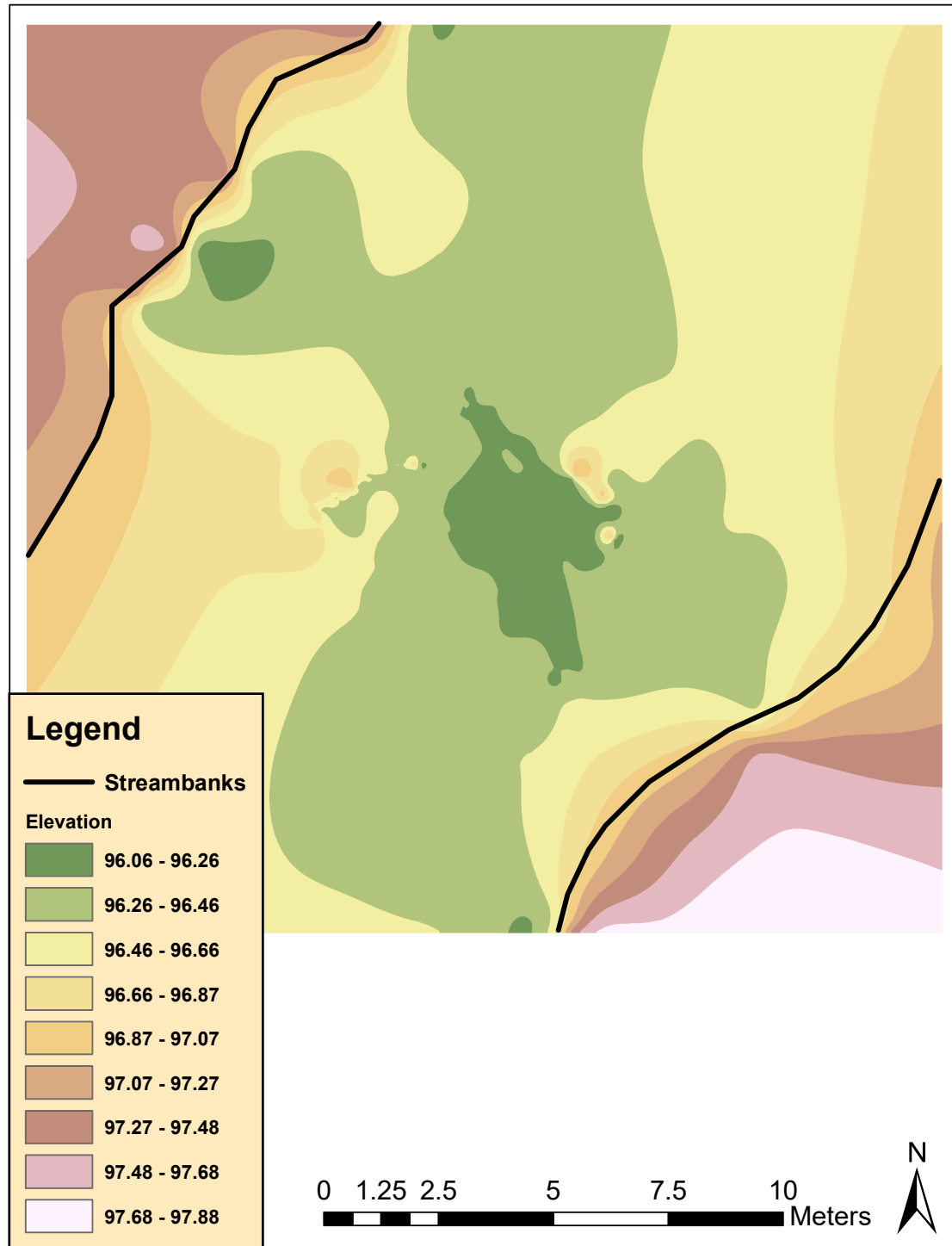


Figure 5. Elevation in ft of Fenton River field site surrounding topography and streambed bathymetry in 2018 at 1.8 m³/s river discharge.

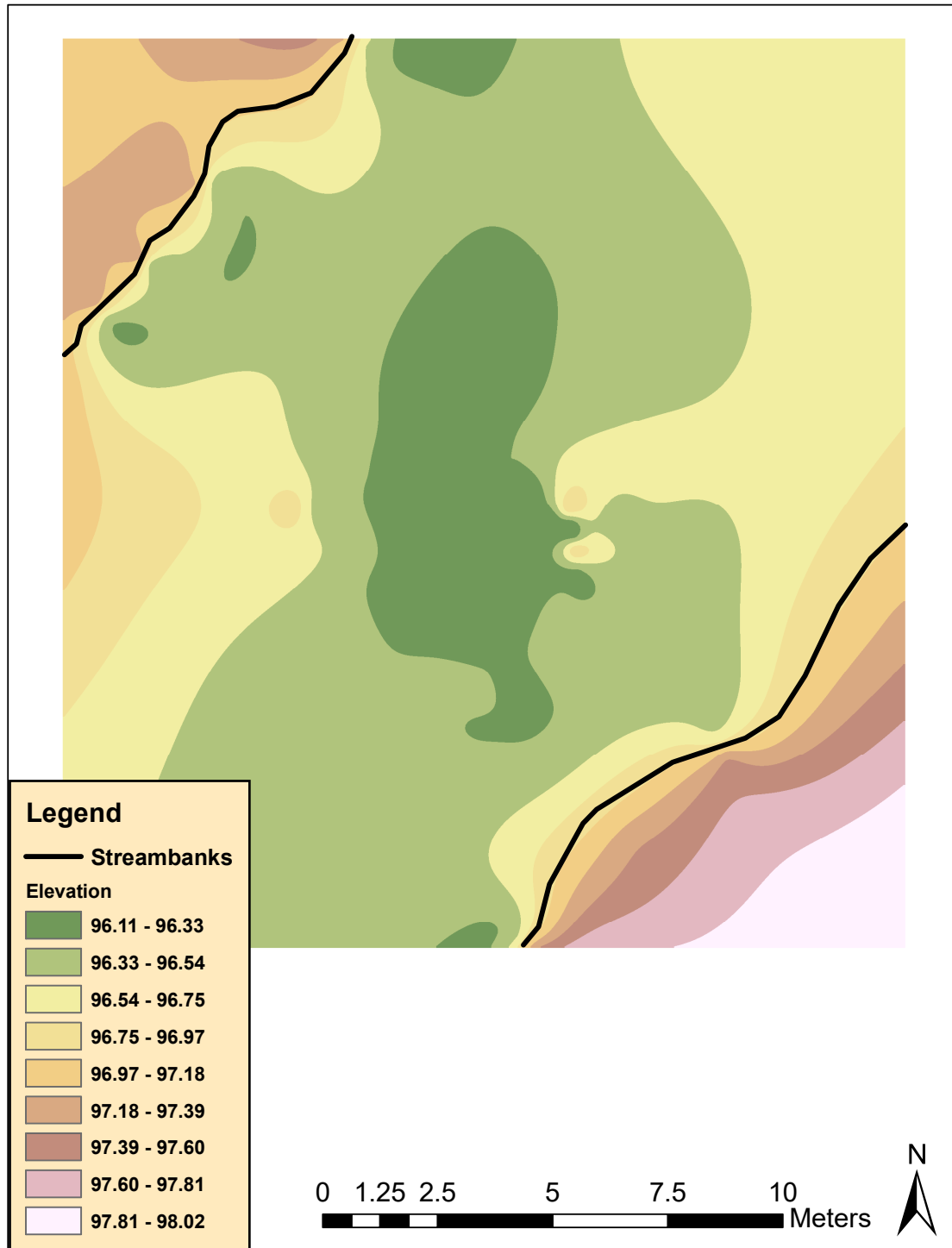


Figure 6. Elevation in ft of Fenton River field site surrounding topography and streambed bathymetry in 2019 at 0.4 m³/s river discharge.

3.2 Cold Water Discharge

The temperature data collected through time using the FO-DTS cable was spatially characterized using the total station, and depicted in ArcMap for each of the different stream discharge days. The temperature data represented by each dot in the figures below is the temperature at the position along the FO-DTS cable averaged throughout the timespan the groundwater injection was active. For the high flow discharge day, $1.8 \text{ m}^3/\text{s}$, the cable collected data for five hours, and the data used was averaged over the time frame the pump was running (2 hours). For the medium flow discharge day, $1.0 \text{ m}^3/\text{s}$, the cable collected data also for five hours, of which all five hours were used because the pump ran the whole time. Data for the low flow discharge day, $0.4 \text{ m}^3/\text{s}$, was not collected until July 2019 due to an unusually wet late summer/early fall. The FO-DTS cable collected data for 4 hours, but due to technical difficulties with the pump, the pump was not running the whole time and the data was averaged over a shorter time span. A cold water pulse was still detected by the fiber optic cable in that timeframe, which is expected as the dye injections indicated it took less than approximately 5 min to establish the groundwater plume once pumping began.

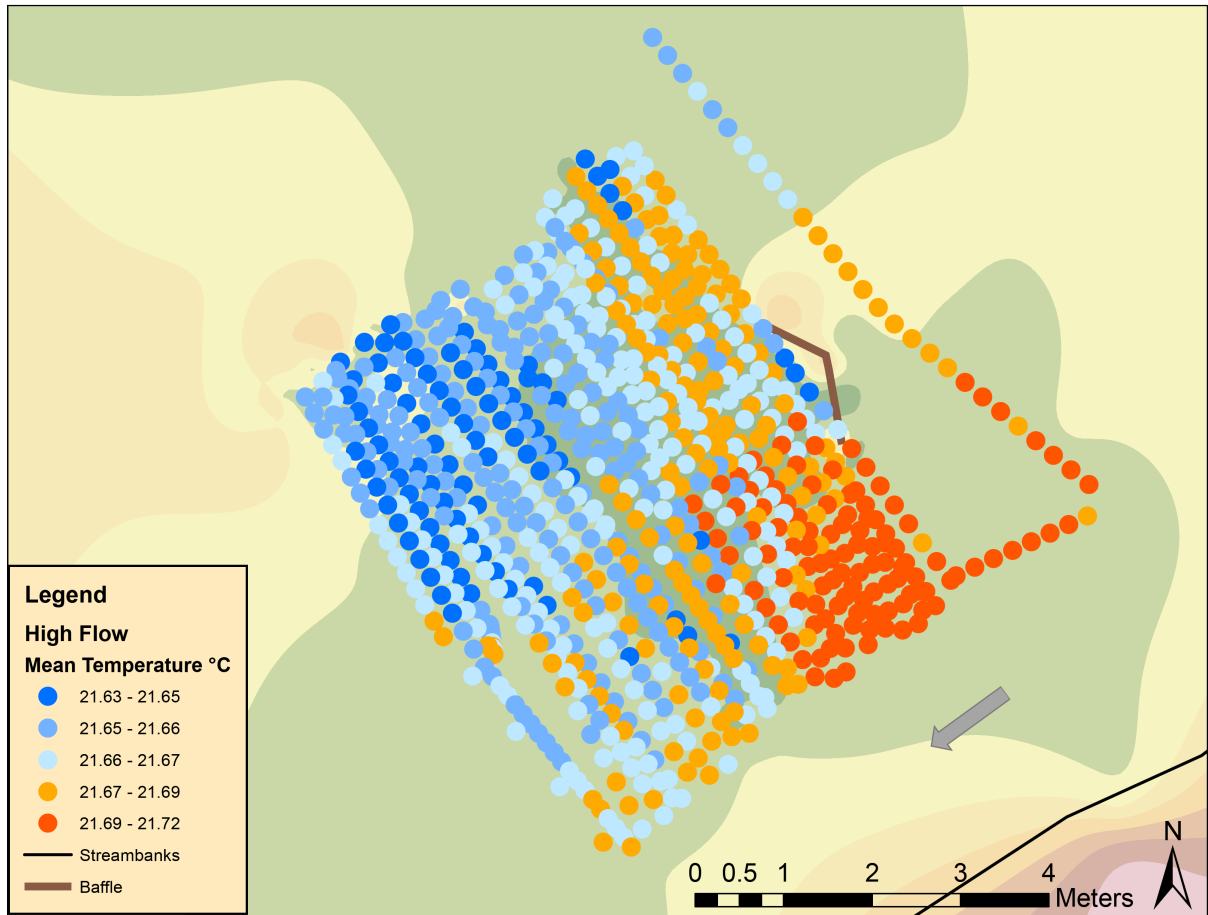


Figure 7. FO-DTS cable collected temperature data through time on the 1.8 m³/s discharge day (high flow), represented by each colored point. It is overlaid on the 2018 bathymetry of the streambed. The arrow indicates stream flow direction.

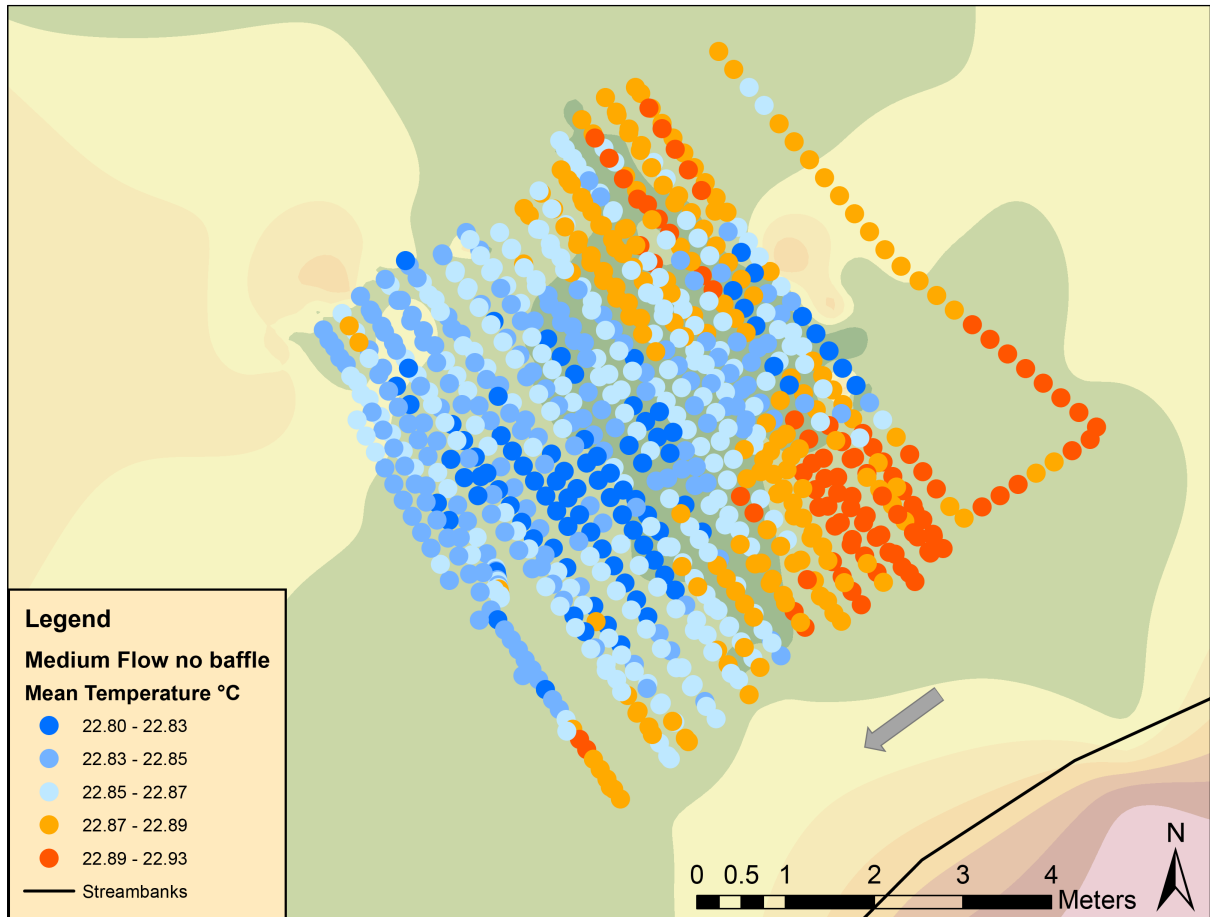


Figure 8. FO-DTS cable collected data on the 1.0 m³/s discharge day (medium flow), overlaid on the 2018 bathymetry of the streambed. The arrow indicates stream flow direction.

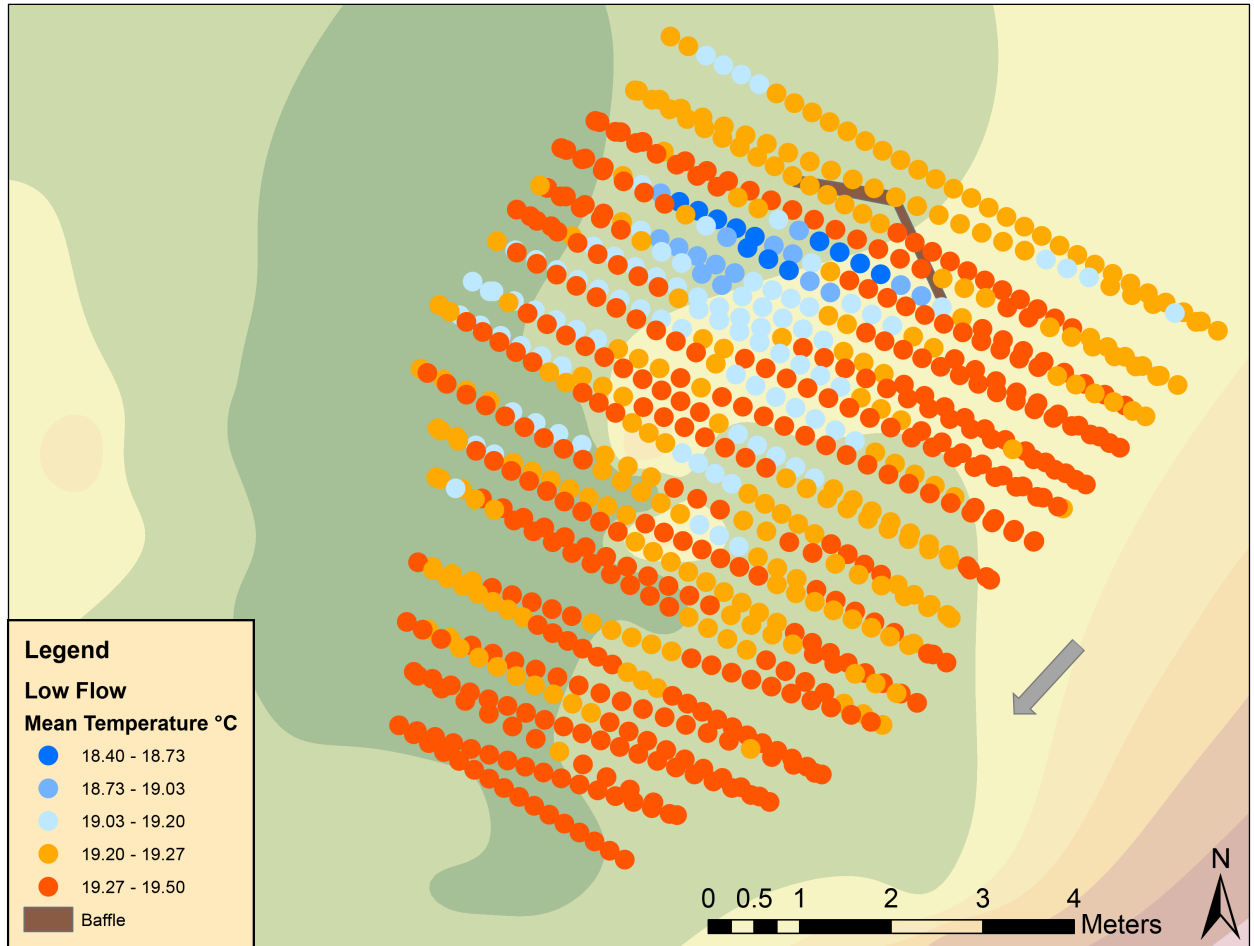


Figure 9. FO-DTS cable collected data from 0.4 m³/s discharge day (low flow), overlaid on the 2018 bathymetry of the streambed. The arrow indicates stream flow direction.

The FO-DTS cable also collected spatial temperature data for the variable rate pump tests, which were mapped in ArcMap. For the first of these tests, at 11.4 L/min (3 gal/min), the FO-DTS cable temperature data was collected over a 50 minute period of pumping at this rate. For the second test, at 18.9 L/min (5 gal/min), the FO-DTS cable collected data as the pump ran at this rate for 10 minutes. At the same pumping rate, but with the slotted distributed release pipe covered in cobbles and streambed substrate, the FO-DTS cable collected data again for 10 minutes. For the highest rate pumping test,

22.7 L/min (6 gal/min), the FO-DTS cable collected data at this rate for 10 minutes.

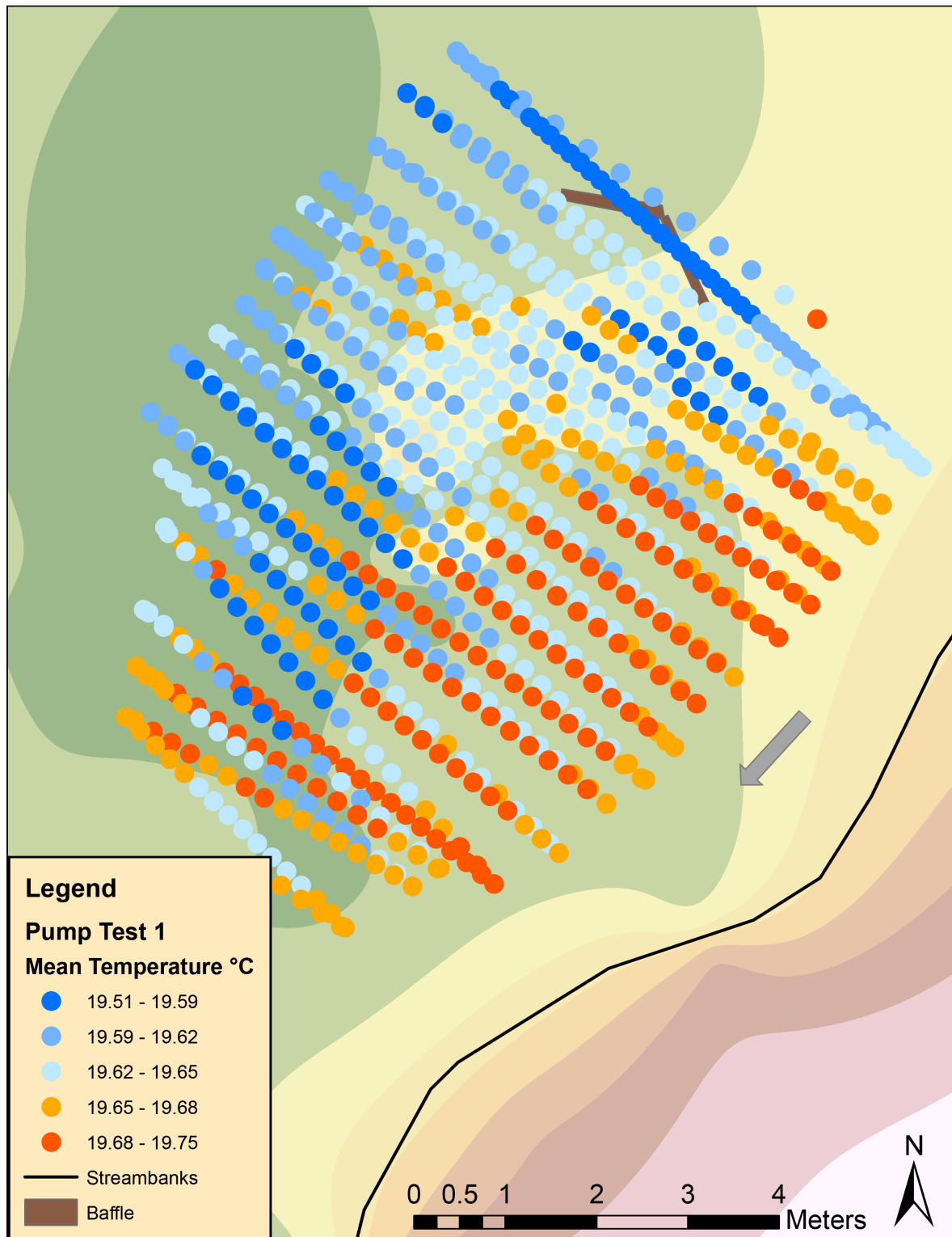


Figure 10. Cold-water plume created by pumping at 11.4 L/min, as depicted by FO-DTS

cable temperature data averaged over time, overlaid on 2019 Fenton river bathymetry.

Arrow indicates stream flow direction.

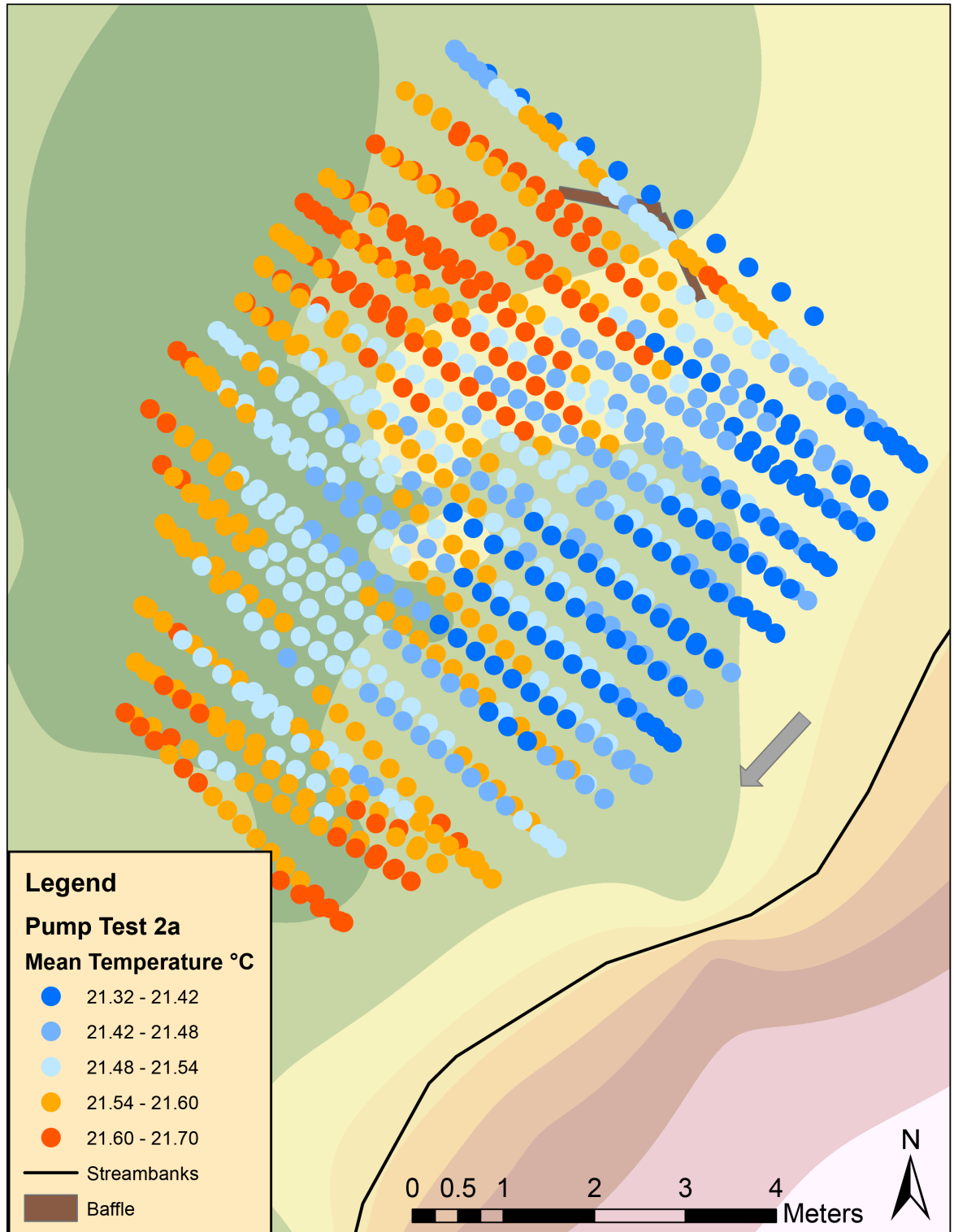


Figure 11. Cold-water plume created by pumping at 18.9 L/min, as depicted by FO-DTS cable temperature data averaged over time, overlaid on 2019 Fenton river bathymetry. Arrow indicates stream flow direction.

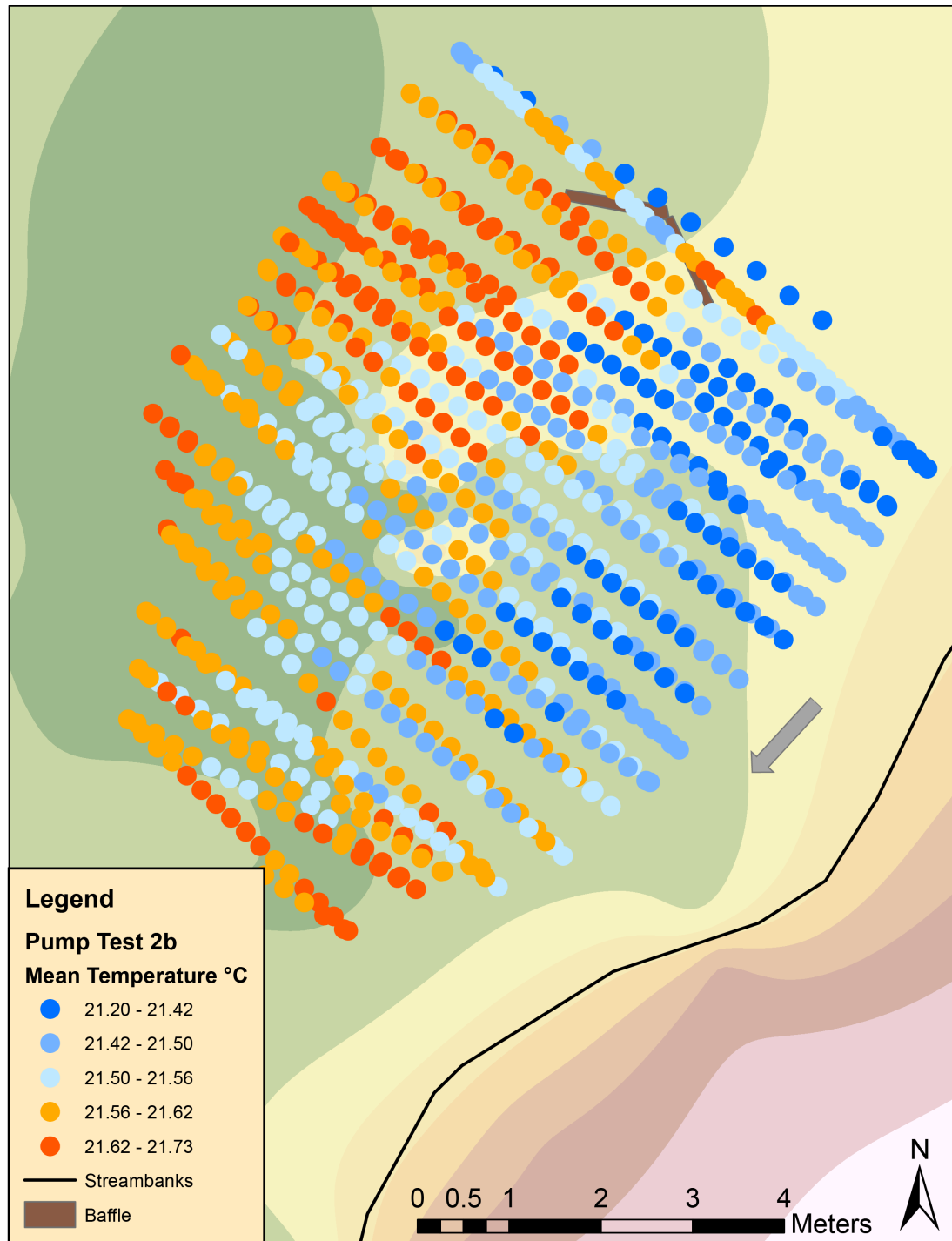


Figure 12. Cold-water plume created by pumping at 18.9 L/min with distributed release pipe buried in large cobbles and substrate, as depicted by FO-DTS cable temperature data averaged over time, overlaid on 2019 Fenton river bathymetry. Arrow indicates stream flow direction.

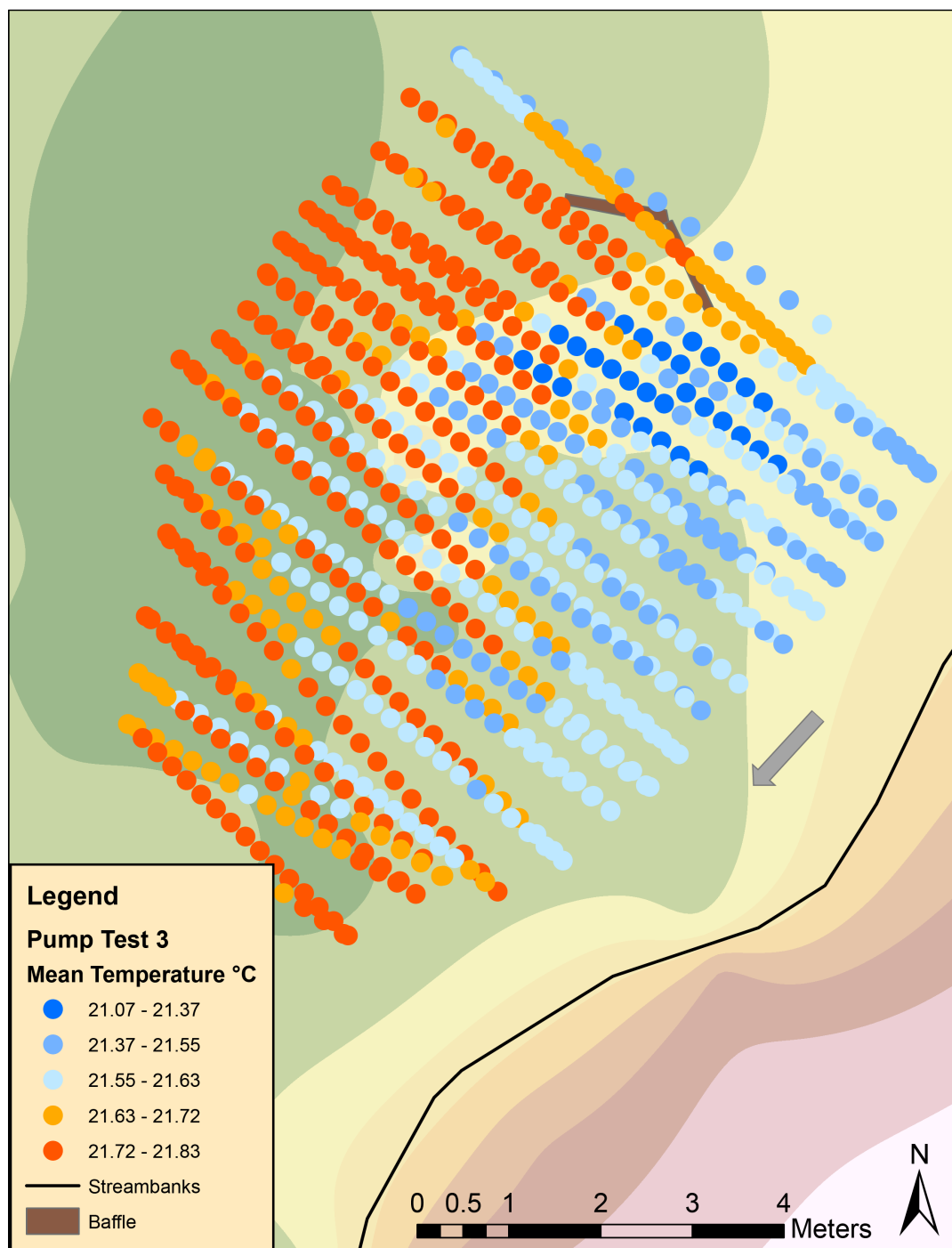


Figure 13. Cold-water plume created by pumping at 22.7 L/min, as depicted by FO-DTS cable temperature data averaged over time, overlaid on 2019 Fenton river bathymetry. Arrow indicates stream flow direction.

In addition to mapping the temperature variation detected by the FO-DTS cable, figures were created of the difference at each point of mean temperature along the cable from the mean background temperature (outside of the discharge zone) of the stream for each experiment. The positive values represent temperature data collected that were greater than the ‘background’ mean temperature, and are all represented in the plots below by a zero value. The negative values represent temperature data that were less than the background, and thus the largest negative values represent the coldest portions of the plume for each experiment.

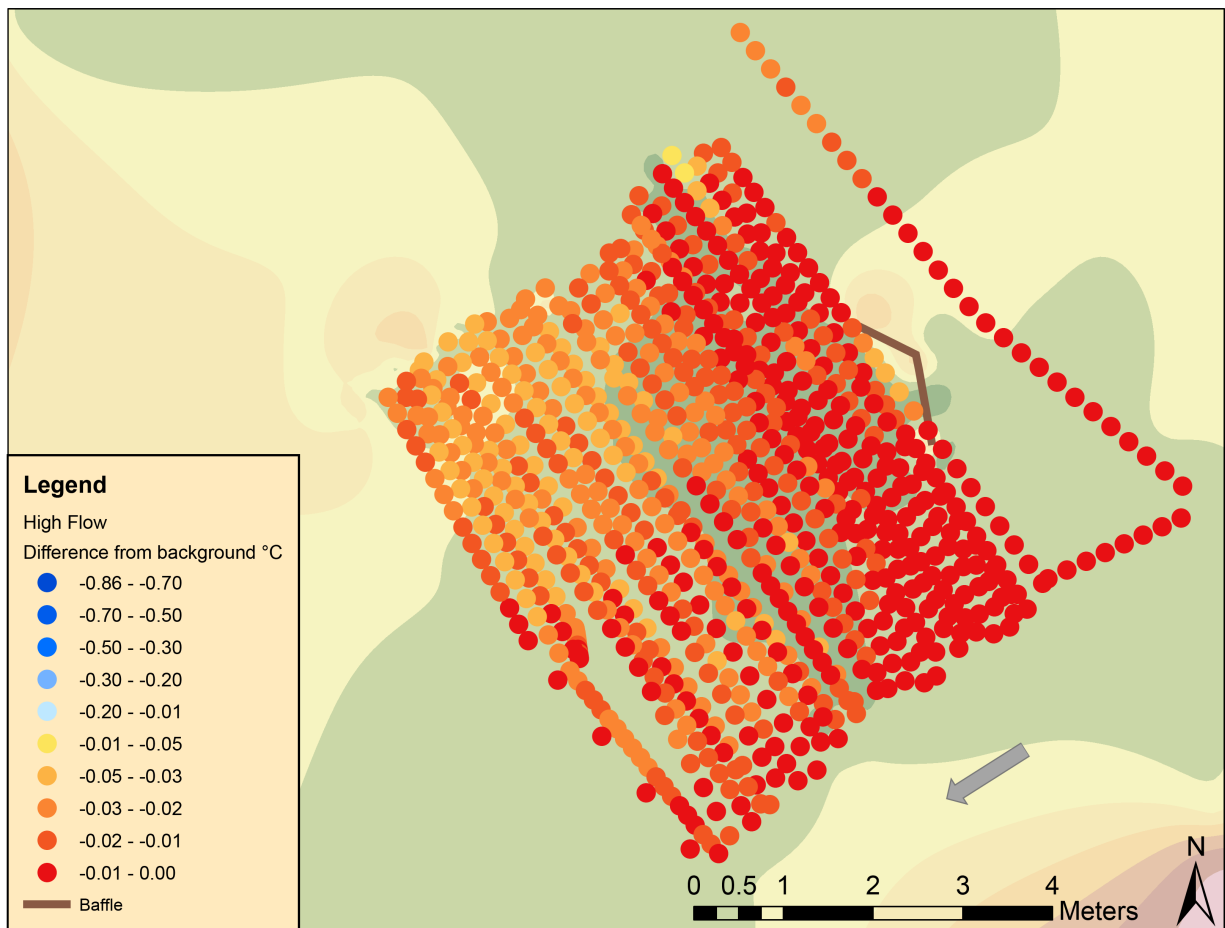


Figure 14. Difference from background temperature in °C at high flow stream discharge ($1.8 \text{ m}^3/\text{s}$) at each point along the fiber optic distributed temperature sensing cable. Arrow

indicates flow direction.

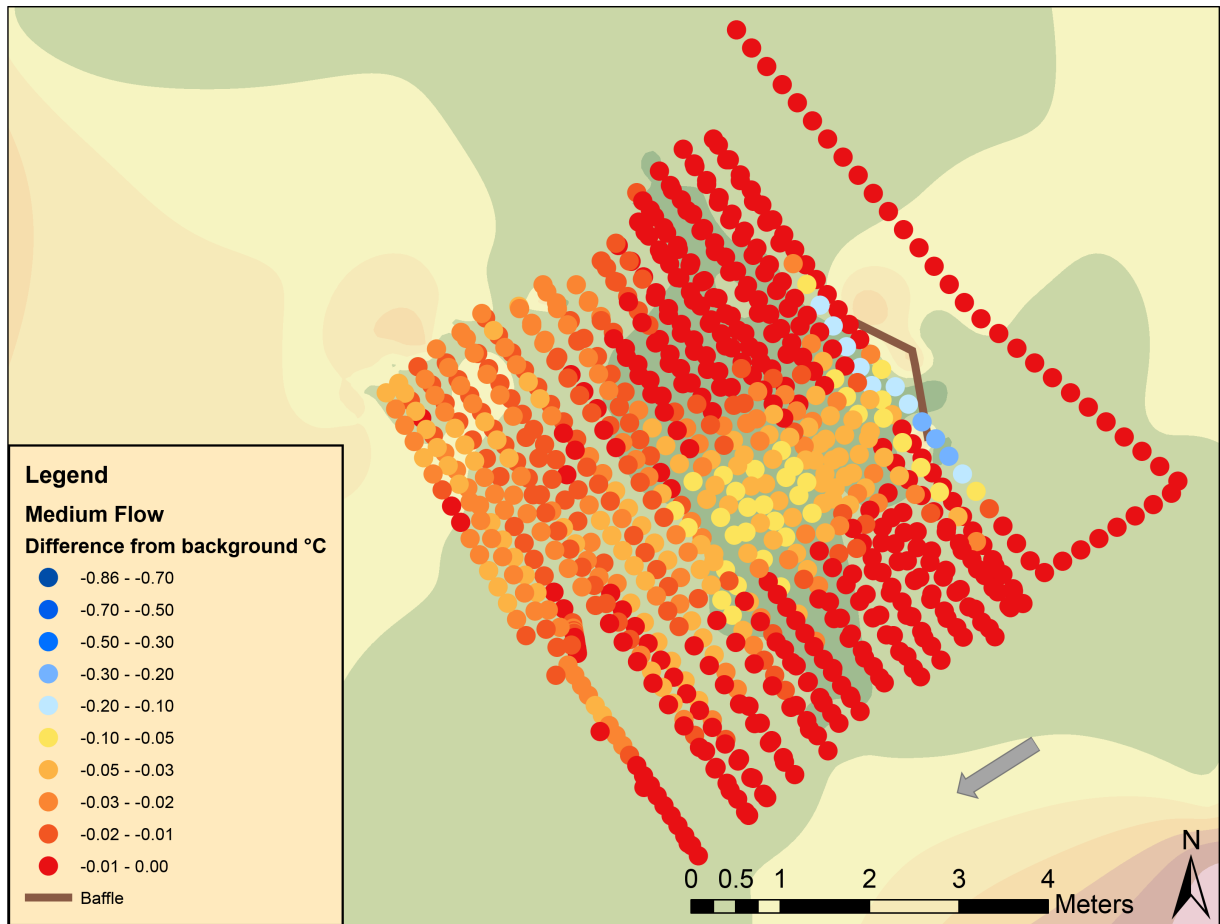


Figure 15. Difference from background temperature in °C at medium flow stream discharge ($1.0 \text{ m}^3/\text{s}$) at each point along the fiber optic distributed temperature sensing cable. Arrow indicates flow direction.

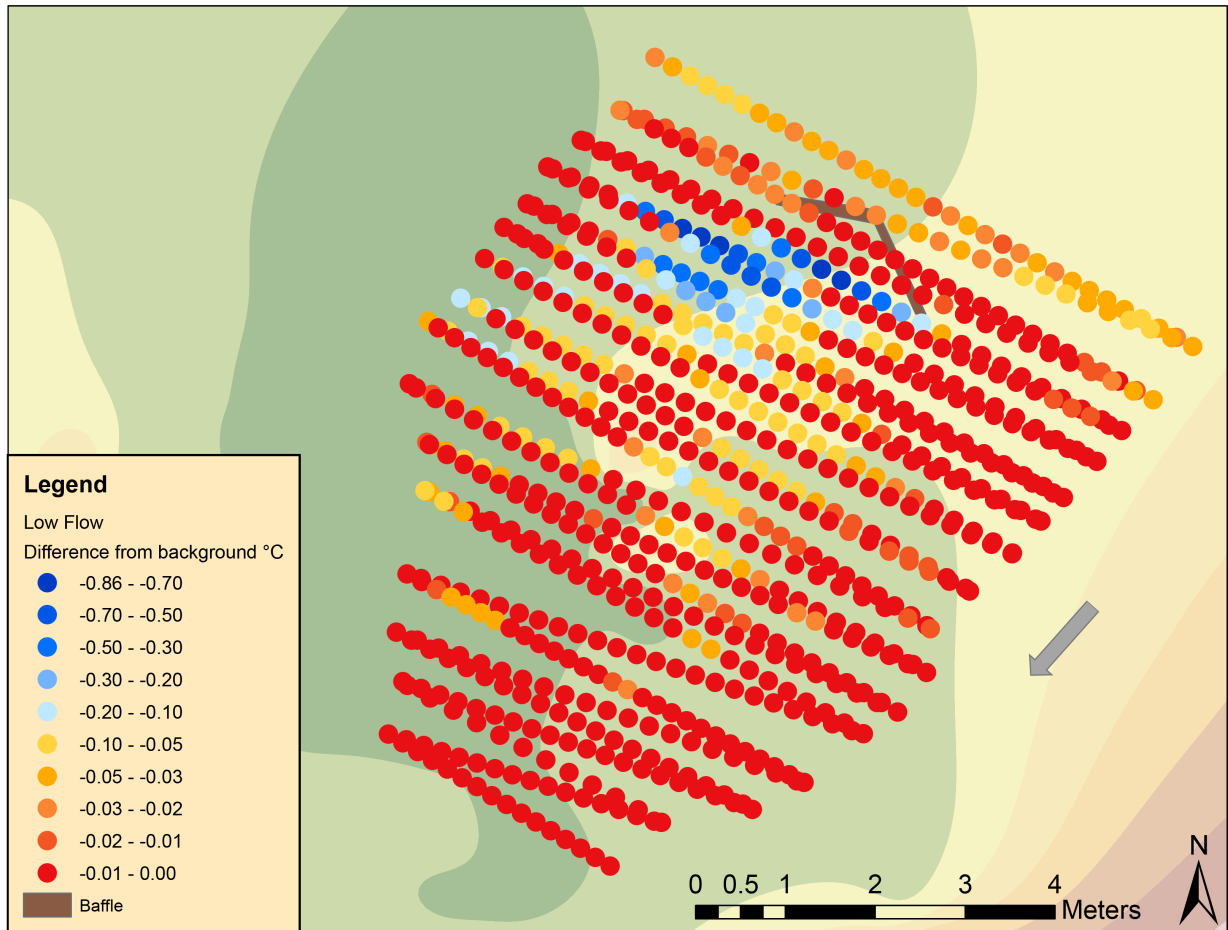


Figure 16. Difference from background temperature in °C at low flow stream discharge ($0.4 \text{ m}^3/\text{s}$) at each point along the fiber optic distributed temperature sensing cable. Arrow indicates flow direction.

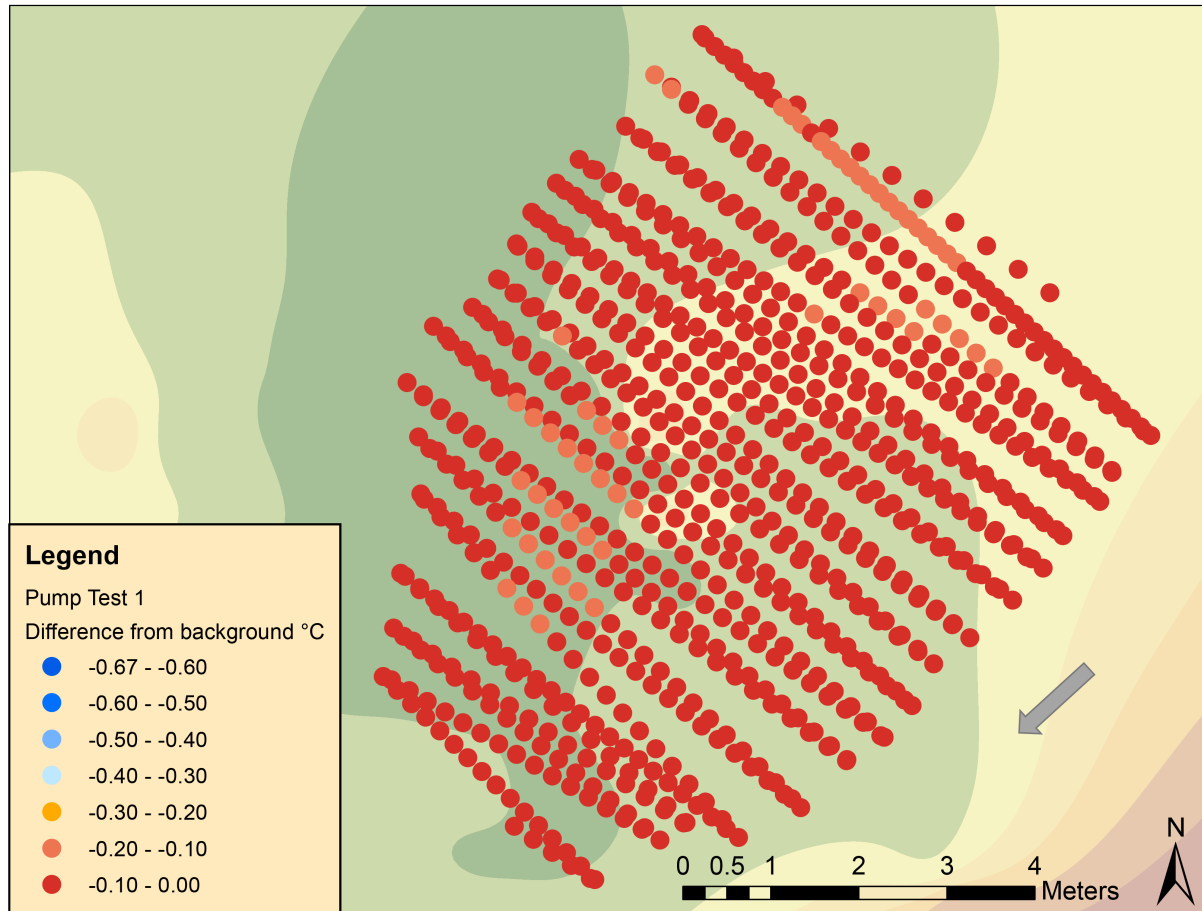


Figure 17. Difference from background temperature in °C at low flow stream discharge ($0.4 \text{ m}^3/\text{s}$) during the first pump test (pumping at rate $11.4 \text{ L}/\text{min}$). Arrow indicates flow direction.

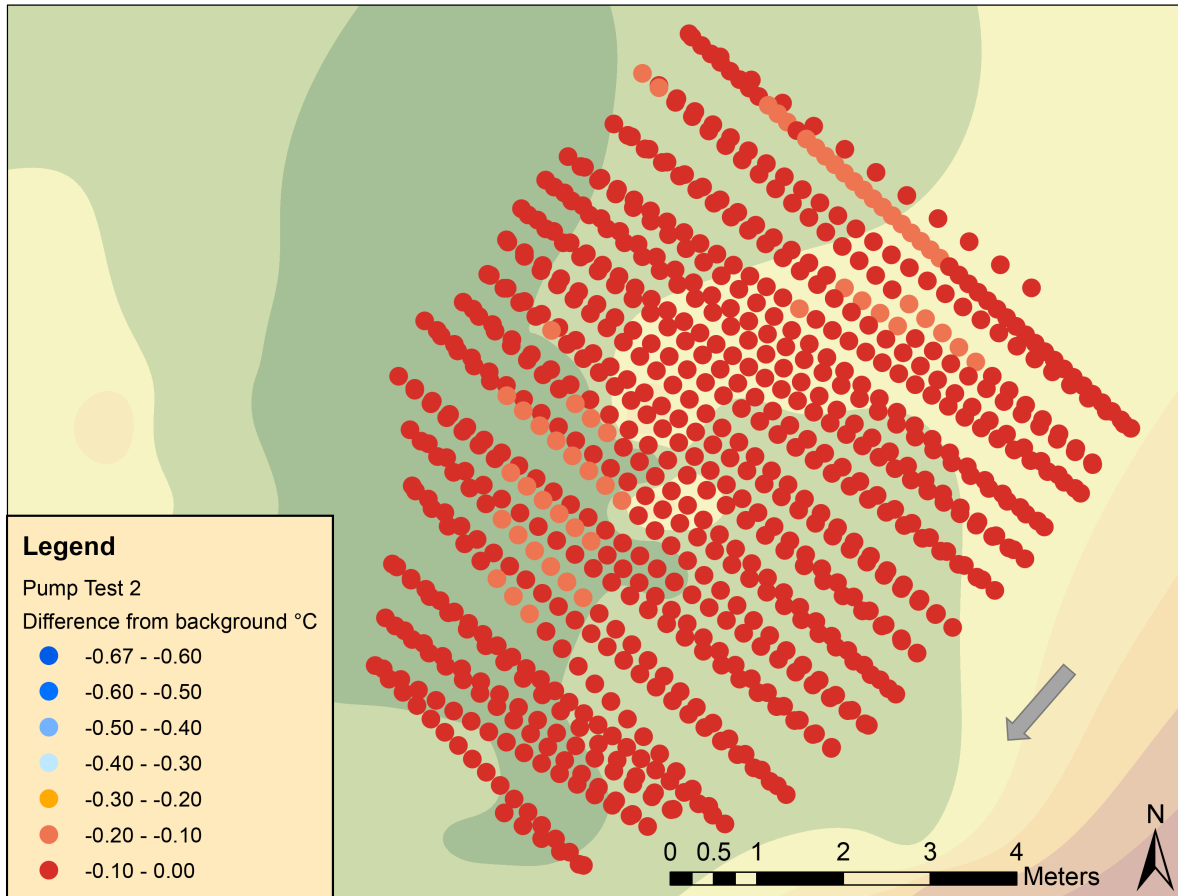


Figure 18. Difference from background temperature in °C at low flow stream discharge ($0.4 \text{ m}^3/\text{s}$) during the second pump test (pumping at rate $18.9 \text{ L}/\text{min}$). Arrow indicates flow direction.

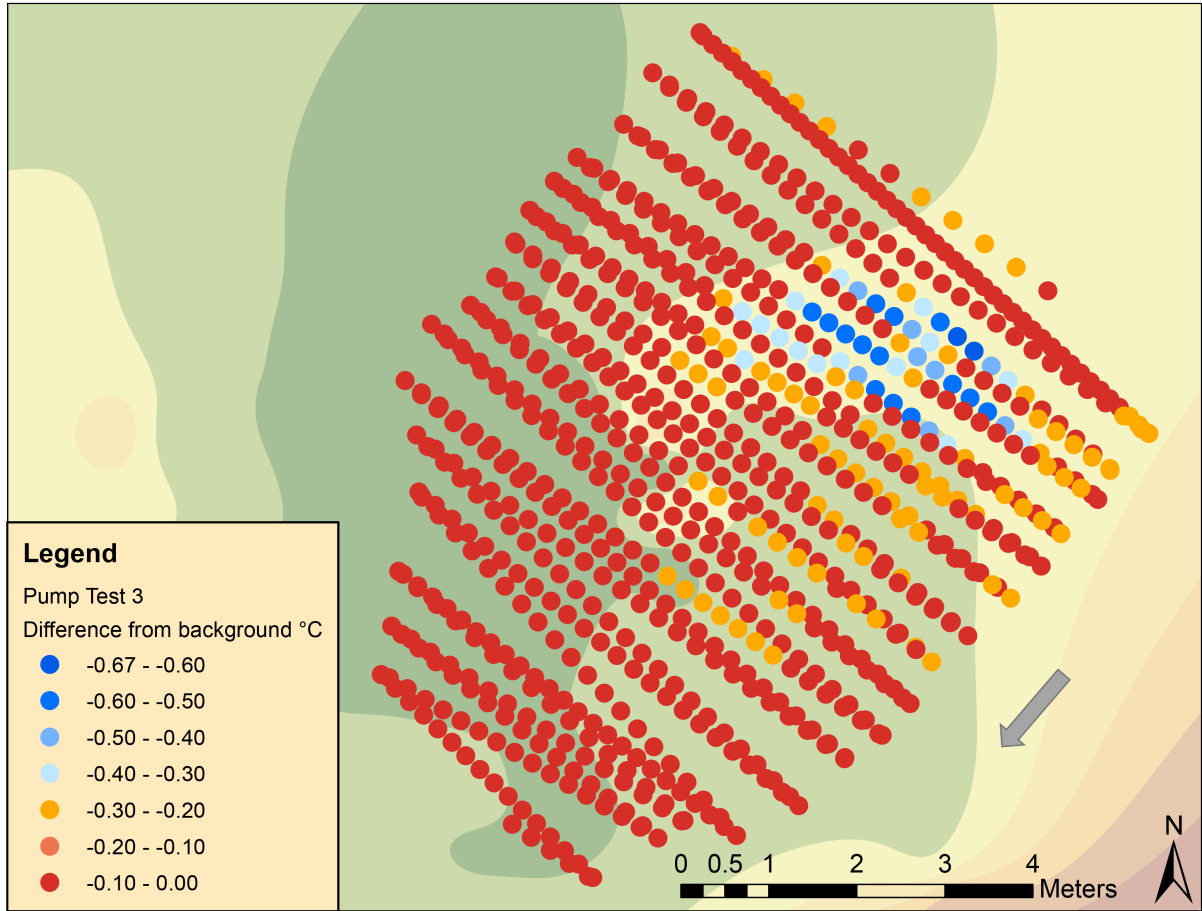


Figure 19. Difference from background temperature in °C at low flow stream discharge ($0.4 \text{ m}^3/\text{s}$) during the third pump test (pumping at rate $22.7 \text{ L}/\text{min}$). Arrow indicates flow direction.

Table 3 shows the overall change in temperature during each of the pump tests, and each of the varying stream discharge rate experiments. The greatest changes in temperature indicate the method used was most successful at lowering the stream temperature. ΔT Mean represents the change in temperature between the coldest mean temperature observed and the warmest mean temperature observed at a point along the FO-DTS cable. ΔT Min represents the change in temperature between the coldest minimum temperature observed and the warmest minimum temperature observed, and

ΔT Mean* represents the change in temperature between the mean background temperature and the coldest mean temperature observed.

	ΔT Mean	ΔT Min	ΔT Mean*	ΔT Max
High flow (1.8 m ³ /s)	0.09 °C	0.24 °C	0.05 °C	0.8 °C
Medium flow (1.0 m ³ /s)	0.31 °C	0.42 °C	0.24 °C	0.9 °C
Low flow (0.4 m ³ /s)	1.1 °C	1.45 °C	0.86 °C	1.2 °C
Pump test 1 (11.4 L/min)	0.24 °C	0.26 °C	0.17 °C	1.0 °C
Pump test 2 (18.9 L/min)	0.38 °C	0.71 °C	0.27 °C	1.3 °C
Pump test 3 (22.7 L/min)	0.76 °C	0.81 °C	0.67 °C	1.5 °C
*difference from mean background temperature				Based on infrared images

Table 3. Change in temperature based on the temperature mean (ΔT Mean), change in temperature between the greatest and least minimum temperatures (ΔT Min), and change in temperature between the background mean temperature and the coldest mean temperature (ΔT Mean*). Change in maximum temperature recorded using the infrared imaging (ΔT Max).

The next form of temperature assessment used to trace the movement of the cold groundwater in the surface water in order to evaluate the extent of the cold-water plume created was thermal infrared imaging, at each of the different overall stream discharges and for each variable pump rate. Natural light images were also taken of the Brilliant Blue dye tracer added to the cold water, and progression photos were taken of the dye as it developed into a full plume.



Figure 20. Brilliant blue dye used as a tracer in cold water, added to hose line.



Figure 21. Images of the dye progression in the groundwater, showing the development of a cold water plume over several minutes of pumping at 23.1 L/min.

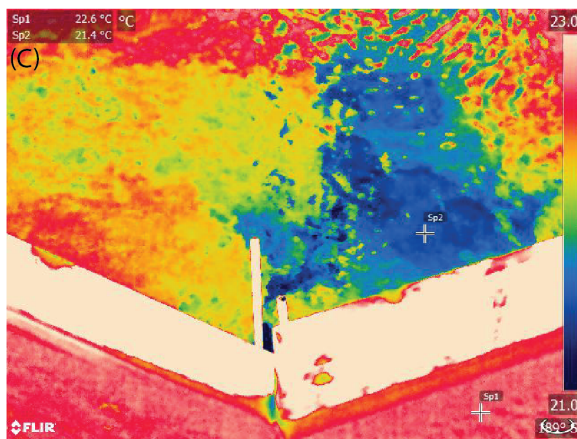
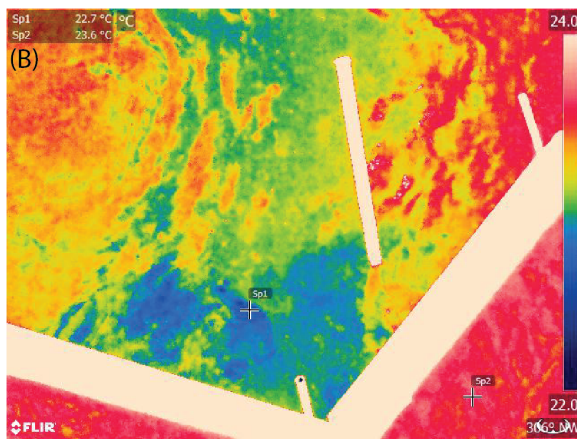
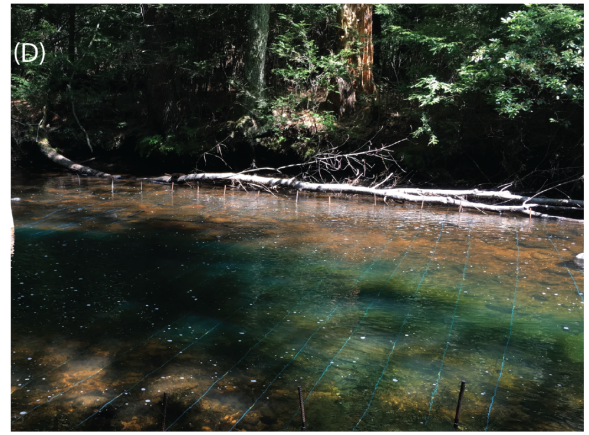
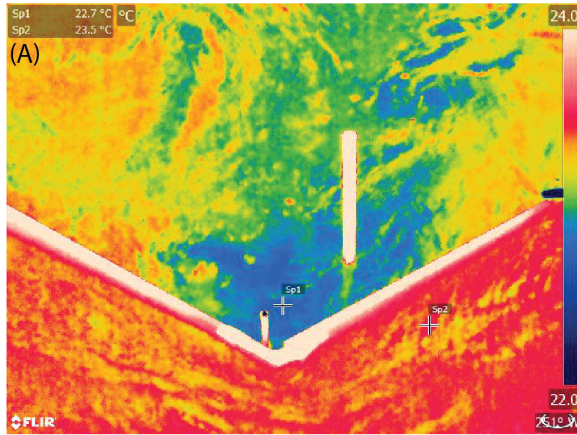


Figure 22. (a-c) thermal infrared images at different stream discharge rates: (a) $1.8 \text{ m}^3/\text{s}$ (b) $1.0 \text{ m}^3/\text{s}$ (c) $0.4 \text{ m}^3/\text{s}$ (d-f) natural light images of blue dye tracer at different discharge rates: (d) $1.8 \text{ m}^3/\text{s}$ (e) $1.0 \text{ m}^3/\text{s}$ (f) $0.4 \text{ m}^3/\text{s}$

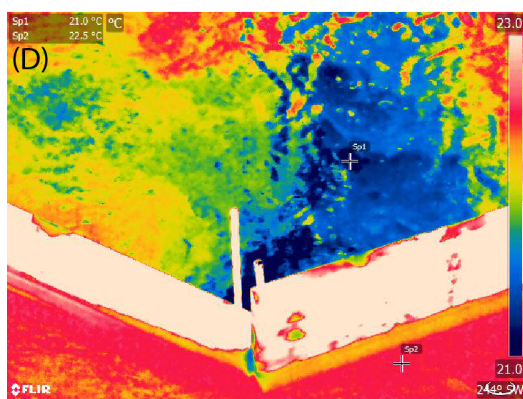
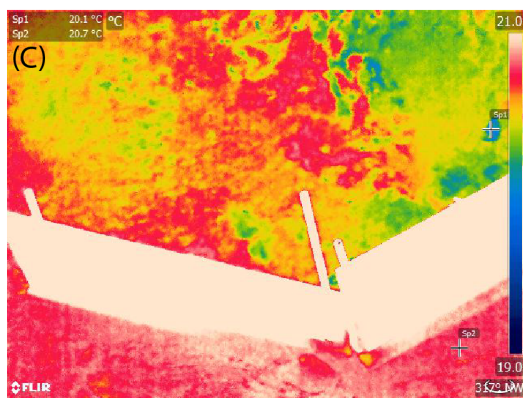
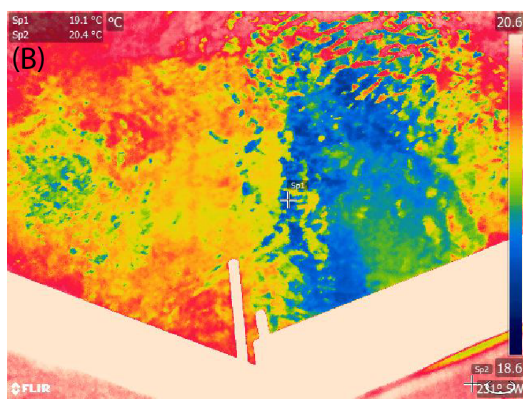
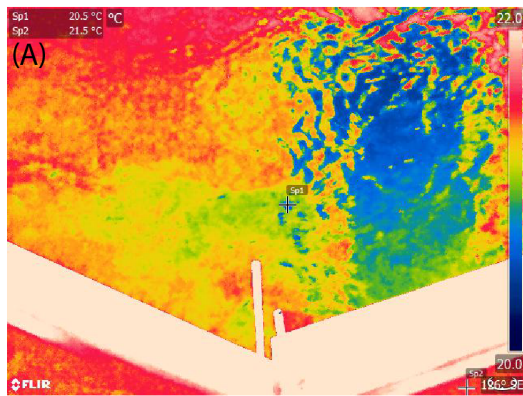
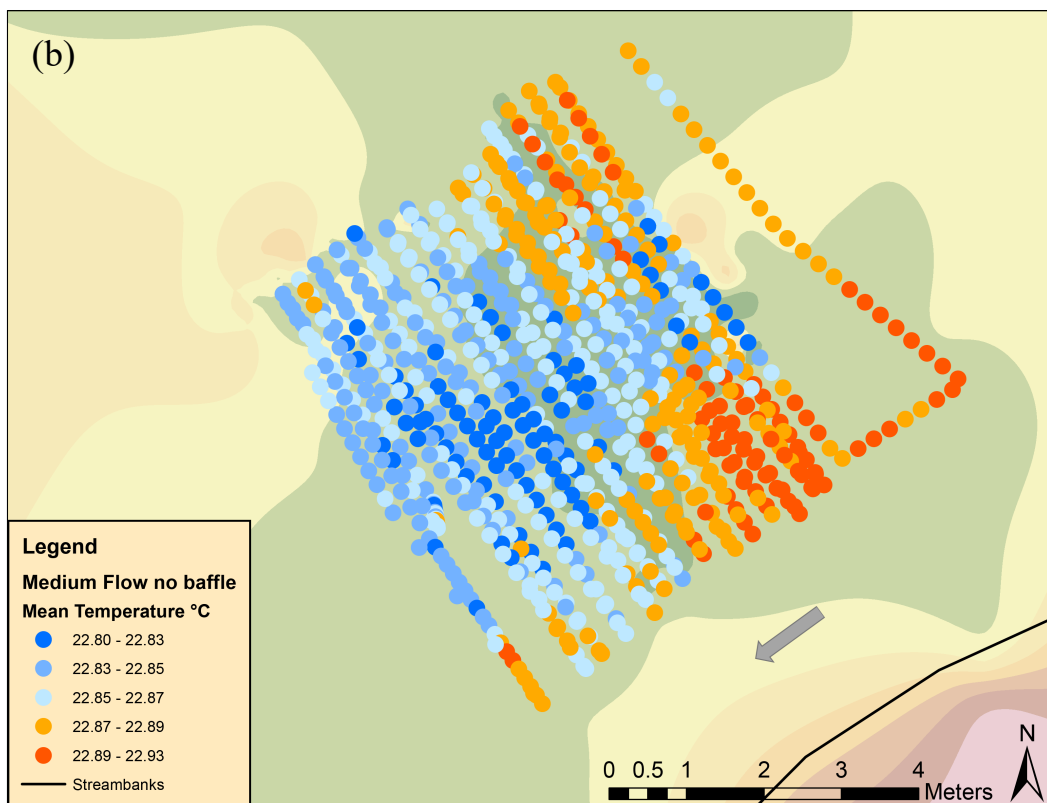
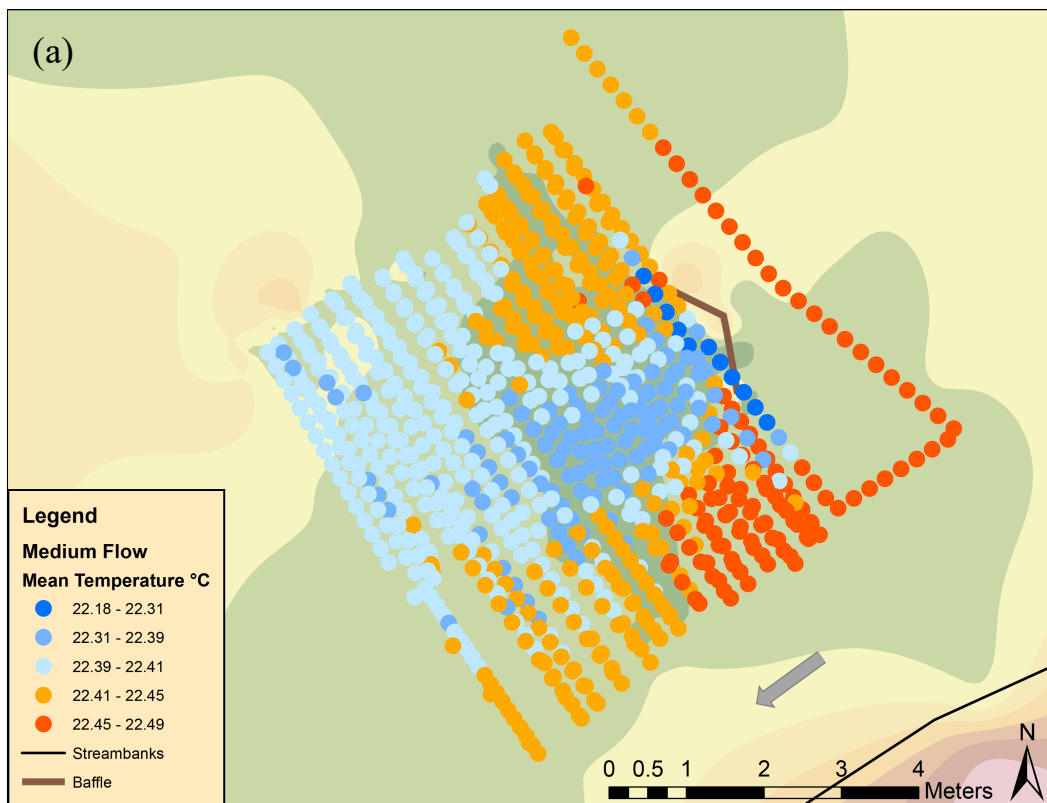


Figure 23. (a-d) Images of infrared at varying pumping rates: (a) 11.4 L/min (b) 18.9 L/min (c) 18.9 L/min with discharge pipe covered in cobbles and stream substrate (d) 22.7 L/min **(e-h)** Natural light images of blue dye tracer during varying pumping rates: (e) 11.4 L/min (f) 18.9 L/min (g) 18.9 L/min with discharge pipe covered in cobbles and stream substrate (h) 22.7 L/min

Next, a velocity vector flow map was created in ArcMap using the velocity (m/s) and direction (degrees) data collected from the handheld Flowtracker ADV. The velocity speed and direction data were spatially correlated using the total station, and interpolations of the speed and direction were created using an IDW (inverse distance weighting) interpolation in ArcMap. The values of these two interpolations were assigned to points in a grid created over the study area, and those points were transformed into vectors that show the magnitude (speed) in their length and direction in the degrees from the values of the interpolation. Velocity data was collected on all three discharge days (1.8 m³/s, 1.0 m³/s, and 0.4 m³/s), and at 1.8 m³/s and 1.0 m³/s flow, velocity data was recorded with and without the baffle present in the stream to determine the effect it has on slowing flow in the study area. Additionally, temperature data from the FO-DTS cable was collected on the 1.0 m³/s discharge day with and without the baffle present. Baffle effect on temperature and flow are depicted in the figures below.



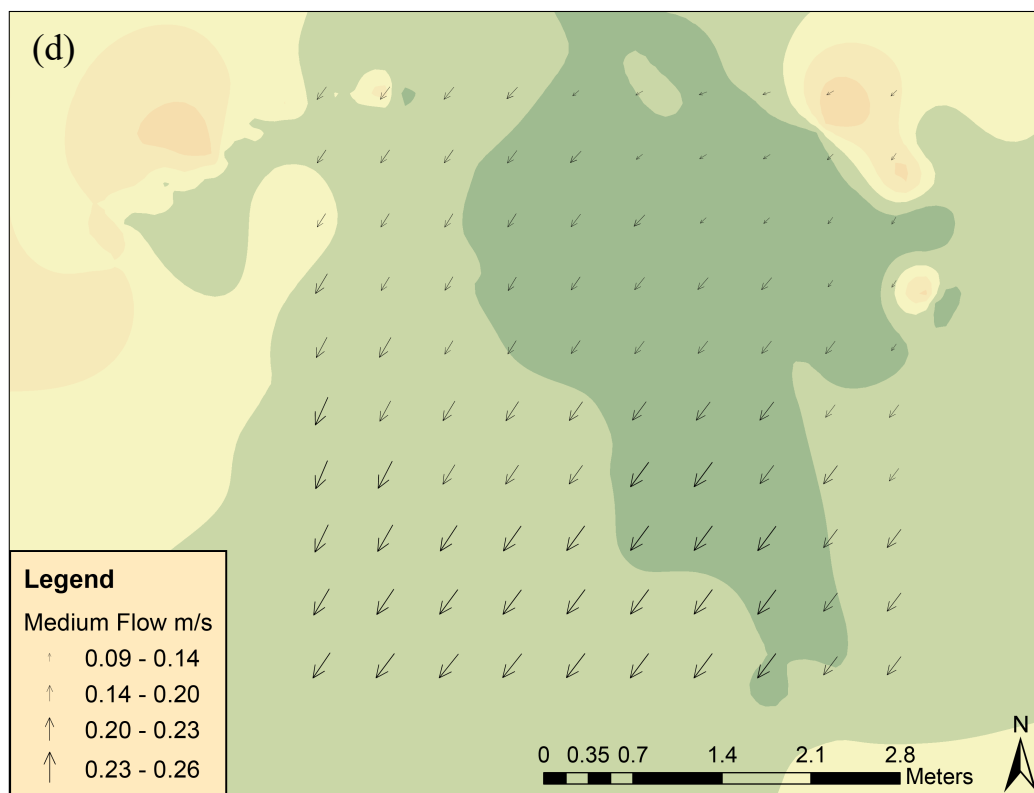
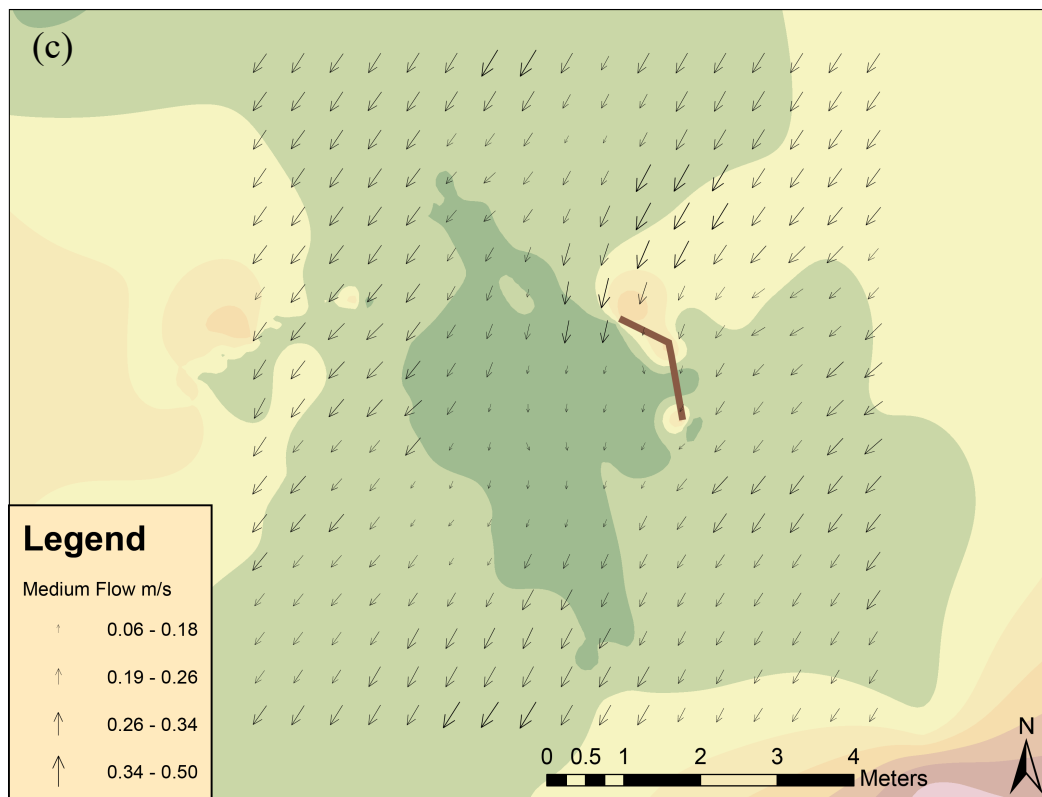


Figure 24. (a and b) Temperature with and without baffle, (c and d) velocity vector flow field with and without baffle present, both at medium stream discharge, 1.0 m³/s.

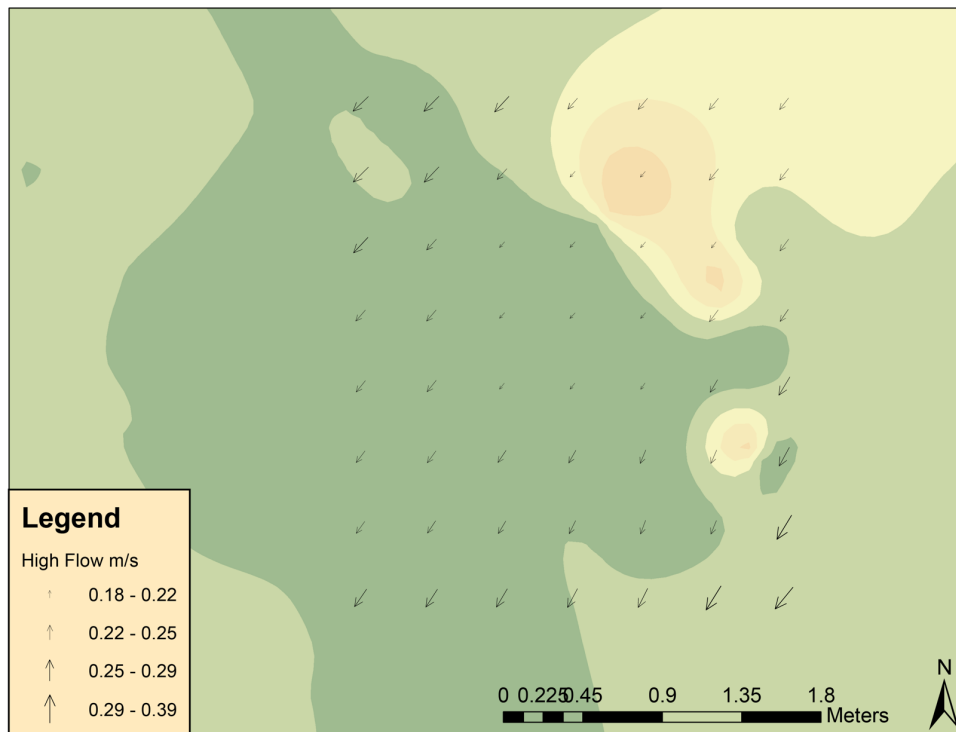
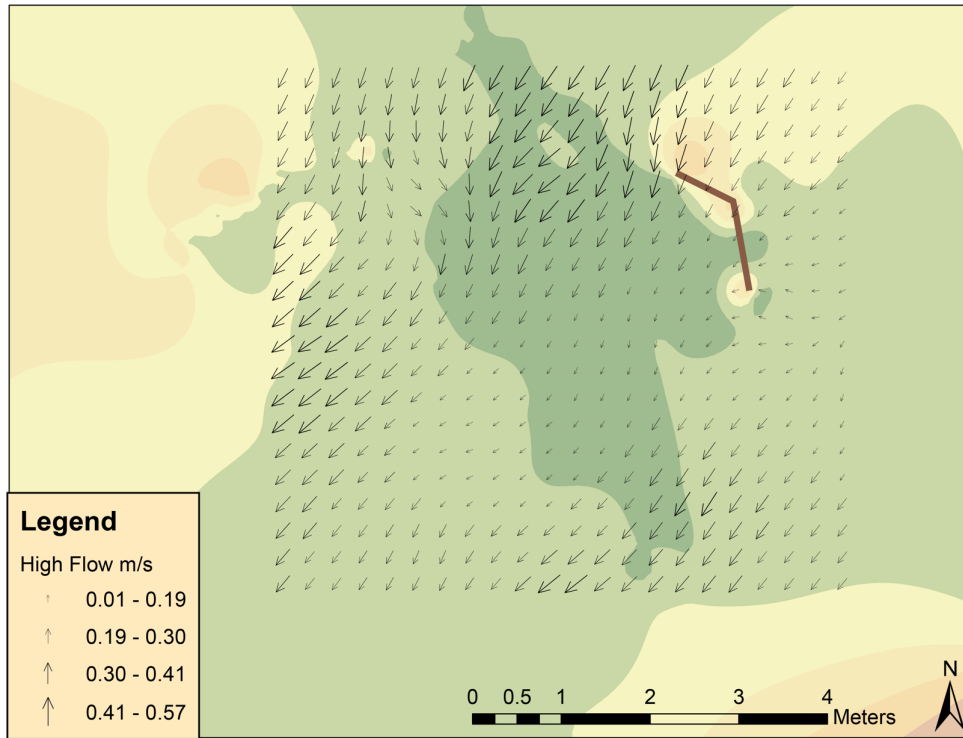


Figure 25. The velocity vector flow-field of the stream at high flow discharge ($1.8 \text{ m}^3/\text{s}$), with and without baffle.

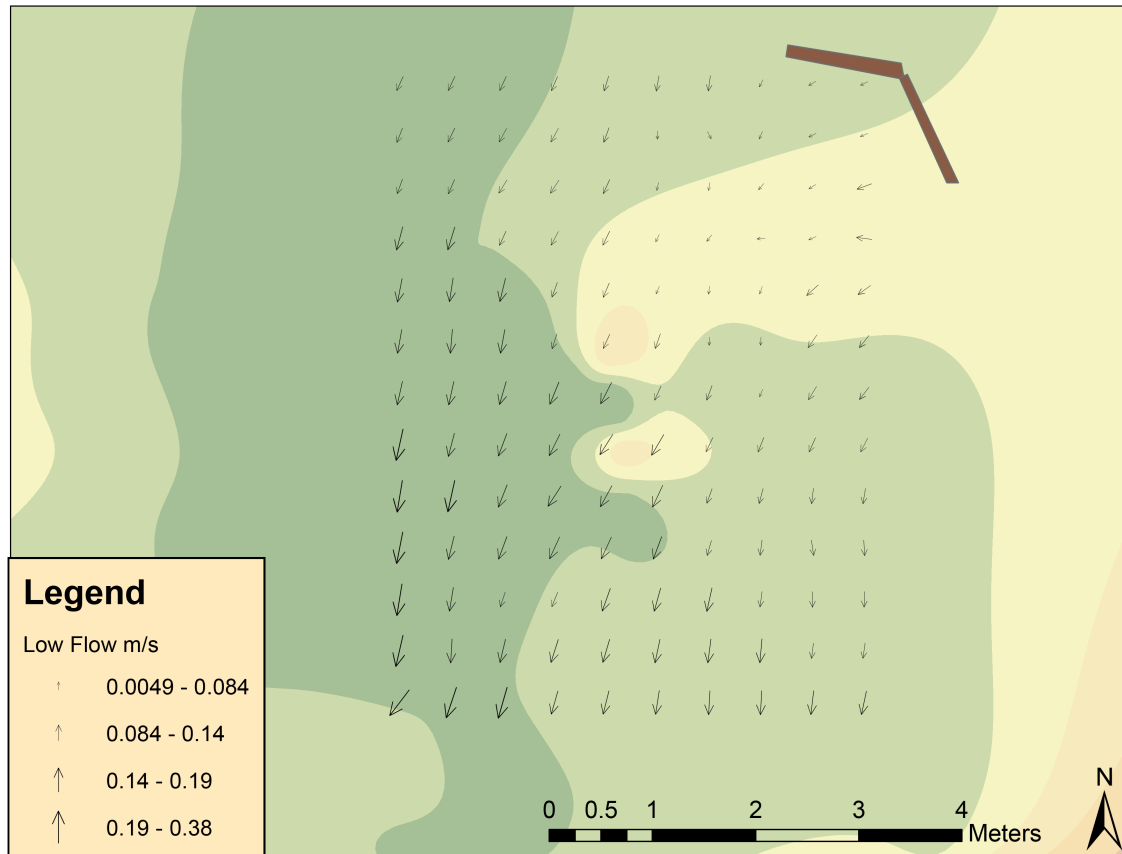


Figure 26. Low flow ($0.4 \text{ m}^3/\text{s}$) velocity vector field with baffle.

DISCUSSION

After assessing the extent and magnitude of the various cold-water plumes created while pumping at typical monitoring well pump rates over a range of natural flow conditions in the Fenton River, it was determined that this active pumping strategy might only provide marginal refuge for cold water fish species in this specific hydrological setting. Despite the appearance of a large blue/cold temperature plume in the thermal maps for the high and medium flow days collected by the FO-DTS cable, the range

between the surface water temperature and the coldest points within the plume for the high flow day ($1.8 \text{ m}^3/\text{s}$) is only a difference of $0.09 \text{ }^\circ\text{C}$, and for the medium flow day ($1.0 \text{ m}^3/\text{s}$), $0.31 \text{ }^\circ\text{C}$ (Table 3). This is further seen in the differences from the background temperature mean (Figures 14-16) which indicate that there is significantly less of a difference from the stream back ground temperature on the high flow and medium flow discharge days. Additionally, the infrared images for high stream discharge ($1.8 \text{ m}^3/\text{s}$) and medium stream discharge ($1.0 \text{ m}^3/\text{s}$) captured a greater temperature difference than detected with the FO-DTS array, showing a change in temperature of $0.8 \text{ }^\circ\text{C}$ for high discharge and $0.9 \text{ }^\circ\text{C}$ for medium discharge (Table 3). While this does show an increase in change in temperature with slower flows, the overall temperature change in the plume is not as dramatic as may be necessary to sustain fish seeking cooler habitat for survival. The lack of a cold-water pocket present at high flow and the limited amount present at medium flow could also be due to the absence of vertical movement of the cold water as it enters the stream reach.

The dye tracer images revealed the cold water was not rapidly mixing with the surface water as it dissipated downstream (Figures 14 and 15), but as a large temperature differential was not picked up by the fiber optic or the infrared images, the cold water may have been highly vertically constrained at mid-depths in the water column. At the lowest stream discharge of $0.4 \text{ m}^3/\text{s}$, an improved thermal plume was created (Figure 9), effectively dropping the surface water temperature by $1.1 \text{ }^\circ\text{C}$ in the coldest portion of the plume, but the change in temperature was still not as dramatic as expected, although a $1.1 \text{ }^\circ\text{C}$ drop in temperature could be useful for fish who live in thermally marginal habitat, where they experience peak temperatures that are only a few degrees over their thermal

thresholds. The infrared images for low flow captured a cold-water plume at the surface, with a change in temperature of $1.2\text{ }^{\circ}\text{C}$ detected (Table 3), and the dye tracer image at low stream flow ($0.4\text{ m}^3/\text{s}$) appears to be a darker shade plume than depicted at high stream flow ($1.8\text{ m}^3/\text{s}$), as seen in Figure 22 (the difference is not discernable between medium and low flows in the natural light dye images). The low stream flow $0.4\text{ m}^3/\text{s}$ experiment showed that this groundwater injection technique is effective at creating a cold-water plume, although only at a difference of ~ 1 degree, and only during base flow conditions.

The variable rate pump tests (performed under low flow discharge conditions) showed that the rate of injection has a small effect on the plume of cold-water created, indicating that an increase in pumping rate creates a slightly cooler plume, but does not make a substantially large difference at an overall stream discharge rate of $0.4\text{ m}^3/\text{s}$ (400 L/s). The slowest pumping rate of 11.4 L/min produced a change in temperature of $0.24\text{ }^{\circ}\text{C}$ between the surface water temperature and the coolest part of the plume detected by the FO-DTS cable (Figure 10 and Table 3), the medium pumping rate of 18.9 L/min produced a temperature drop of $0.38\text{ }^{\circ}\text{C}$ (Figure 11 and Table 3), and the highest pump flow rate of 22.7 L/min created a temperature drop of $0.76\text{ }^{\circ}\text{C}$ (Figure 13 and Table 3). (The low flow discharge experiment at $0.4\text{ m}^3/\text{s}$ was pumped at a rate of 23.1 L/min , with a $1.2\text{ }^{\circ}\text{C}$ change in temperature.) The infrared images captured for each pump test were able to detect a temperature variation at the surface showing an increase in temperature change with increasing pumping rate. For pump test 1 (11.4 L/min), the infrared images showed a change in temperature of $1.0\text{ }^{\circ}\text{C}$, for pump test 2 (18.9 L/min) a change in temperature of $1.3\text{ }^{\circ}\text{C}$, and for pump test 3 (22.7 L/min) a change in temperature was

observed of 1.5 °C (Figure 23 and Table 3). The natural light dye images taken for each different pump test did not show much apparent variation in the size of the plume or the darkness of the color besides between the first pump test (11.4 L/min) and the last (22.7 L/min). This indicates that visual analysis of the plume magnitude and extent based on visual observations is likely not sensitive enough to capture change in groundwater concentration within the water column. Additionally, we hypothesize that even a poorly advectively-mixed groundwater plume will exchange heat with the surrounding channel water via conduction, and the dye would not capture this potentially important heat mixing process.

The variations in groundwater injection techniques were tested by comparing the FO-DTS temperature data and infrared images when the slotted release pipe was placed on the streambed versus when it was covered with cobbles and partially buried, revealing a temperature variation between the two, indicating that covering the discharge pipe to further mimic a natural seep may create a colder plume as it slows the release of cold-water and prevents it from immediately mixing with the surface water. At 18.9 L/min, the uncovered injection pipe produced a temperature drop of 0.38 °C, and at the same rate, with the pipe covered and partially buried, there was a temperature drop of 0.53 °C, as seen in Figures 11 and 12. While the variation is not much, it does indicate that there may be a further decrease in temperature when cold-water is discharged through a buried/covered in substrate pipe. The infrared images and natural light dye photos were not able to detect a difference between the two cold water release configurations (Figure 23).

The velocity vector flow field maps created with and without the baffle present under high and medium flow conditions ($1.8 \text{ m}^3/\text{s}$ and $1.0 \text{ m}^3/\text{s}$) indicated that the baffle does effectively slow the main channel flow and prevent immediate mixing of the surface water with the groundwater. With the baffle present at $1.8 \text{ m}^3/\text{s}$ flow, flow prior to the obstruction is in the $0.41\text{-}0.57 \text{ m/s}$ range and behind and downstream of the baffle the flow slows to $0.01\text{-}0.09 \text{ m/s}$. Similarly, with the baffle present at $1.0 \text{ m}^3/\text{s}$ flow, flow upstream of the baffle is $0.34\text{-}0.50 \text{ m/s}$, and downstream/directly behind the baffle it is $0.06\text{-}0.18 \text{ m/s}$ (Figures 18 and 19). The temperature data collected with the fiber optic cable on the medium flow day ($1.0 \text{ m}^3/\text{s}$), with and without the baffle, also indicated that the baffle improved the temperature drop in the cold-water plume. The temperature map without the baffle showed a temperature change of 0.13°C , and with the baffle a change of 0.31°C , showing that the warmer surface water was most likely delayed mixing with the cooler groundwater, causing the temperature difference in the plume to be greater (Figure 24).

In conclusion, there was a trace of a thermal anomaly showing the potential for creating an effective cold-water pocket under low flow conditions, with a baffle, and at a high pumping rate (22.7 L/min). After a precipitation event, there was hardly a discernable temperature impact from the groundwater injection. The recommendation for future studies would be to incorporate these thermal assessments on a plume injected in a slower flowing area of a stream, along the banks and out of the main channel flow path where the overall velocity is already reduced. A number of stream restoration studies indicate that variables such as streambed topography and grain size, along with height and angle of the baffle used can have a strong effect on the amount of turbulence

produced and slowed flow field created. A study that assessed deflectors placed along adjacent stream banks at 45° (pointing downstream), 90°, and 135° (pointing upstream) found that deflectors were most effective when positioned at the 90° angle in terms of disrupting the flow field (Biron et al. 2004). This study also indicated that turbulence and bed shear stress is at its highest at the tips of deflectors at 90° and 135° (Biron et al. 2004). Additionally, understanding grain size and streambed topography is an important component to designing deflectors for streams, as a smoothed streambed's mean and turbulent flow dynamics vary from a rocky streambed due to a rough streambed's topography increasing streambed friction and resulting in slower flows for a further distance downstream of the deflector (Biron et al. 2005). Bank oriented deflectors have also been found to create a high velocity downstream that can lead to erosion problems and scouring issues if left in the stream permanently (Champoux et al. 2003), which is why this method of creating a cold-water pocket utilized a removable baffle (Kurylyk et al. 2015). Taking stream restoration design factors such as these into account could result in a more significant temperature difference that would be able to be utilized by cold-water adapted fish species attempting to thermoregulate during extreme temperatures. Additionally, it could be suggested that implementation of a similar actively pumped strategy only occur during lowest flow periods of the year in a stream of similar size as the Fenton River.

On a larger scale, augmenting natural thermal refuge can be more effective with greater amounts of thermally heterogeneous water being moved. In rivers that receive effluent from facilities, like nuclear power plants, fish can be found utilizing the large thermal plumes created by the effluent (Neill et al. 1974). The Joint Base Cape Cod

pumps approximately 40 L/s of cooling groundwater (~12 °C) into a 450 L/s river (average flow) in summer, which creates a more effective temperature decrease and larger thermal refuge, as depicted in Figure 27. Also, the Furnace Brook tributary confluence within the Housatonic River in Cornwall, CT creates a large, cool area used by trout that is protected from fishing in the summer months due to their reliance on this thermal refuge for alleviating thermal stress (Figure 28). This technique as a climate mitigation strategy might be better suited to large scale operations which empty cold water at a greater scale into stream reaches. The tested method of this research using a common house pump with one well in a small stream may not be a viable option to produce a large enough temperature variation to create an effective thermal refuge.

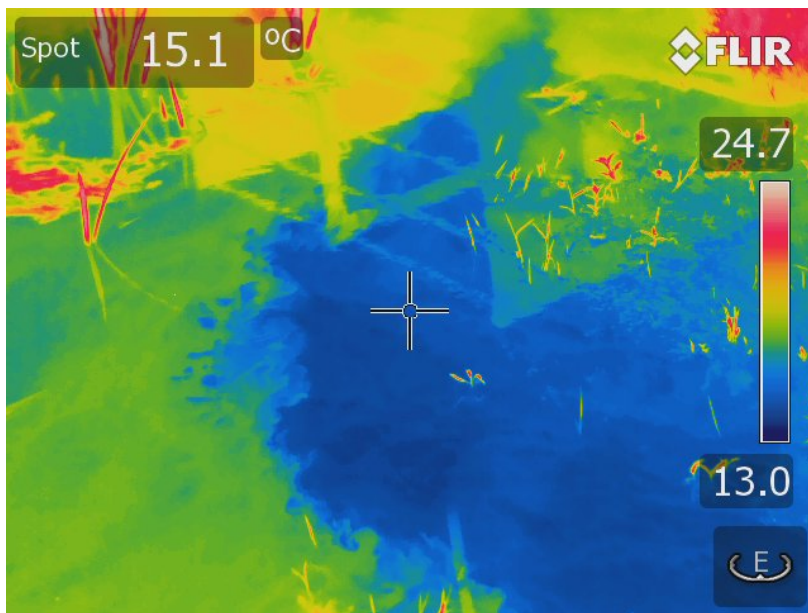
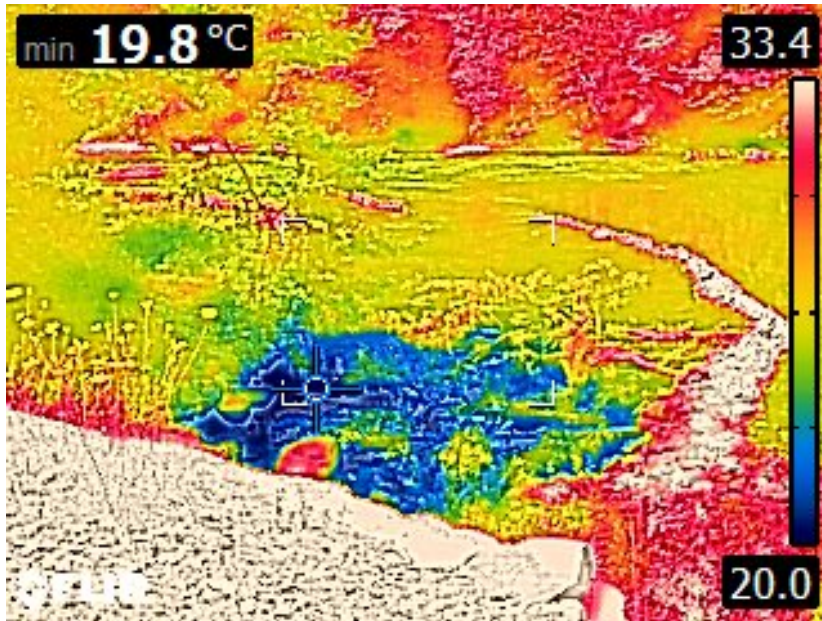


Figure 27. Infrared image of a groundwater pump and treat discharge run by the Joint Base Cape Cod.



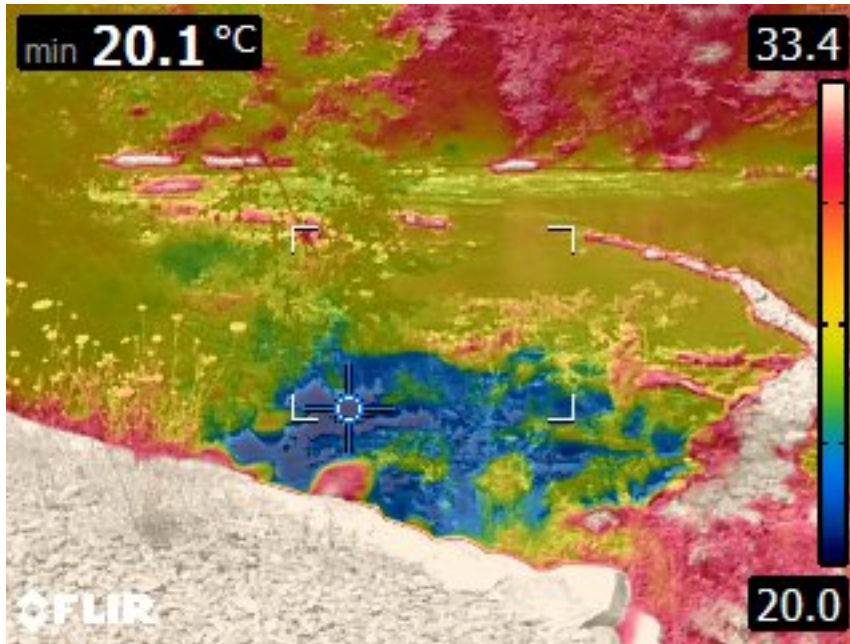


Figure 28. Infrared and natural light images of tributary confluence from Furnace Brook with the Housatonic River, utilized by trout as thermal refuge. Images taken by Christopher Sullivan and Kevin Jackson.

CONCLUSIONS

The results of this study indicate that while thermal refuge are an important natural process that protect aquatic species from exceeding their thermal thresholds, and can create a buffer between species and the effects of climate warming, an engineered solution in a stream of this size and using a common household water supply pump may not be a viable option for augmenting natural thermal refuge in the channel center. As seen by the example of larger scale cold water plume in a smaller stream adjacent to Joint Base Cape Cod (Figure 27). Active pumping may be a workable solution for species seeking thermal alleviation by using large pumped volumes in lower stream flow settings. But at the small scale in a river the size of the Fenton, pumping at rates of 23.1 L/min

from a nearby well, this method may only be effective at low flows, and is not reliable for dropping the surface water temperature more than a few degrees. This technique could be found useful for areas where the surface water temperature exceeds thermal thresholds by only a degree or two, at low flow periods of the summer. In instances where only a small buffer is needed, this could be a viable option. Additional elements of cold-water injection methods and the usage of a flow obstruction device, like a baffle, can improve the refuge created by preventing the groundwater from immediately mixing with the surface water. The slotted distributed release pipe helped with this, along with burying it in the substrate, to create a more seep-like injection method. The baffle also proved to be effective at disrupting the main channel flow enough to create a slower flow field behind the wooden boards for a more ideal injection location. Future work could include different baffle configurations, including using natural restoration materials for the baffle components and setting up the baffle in the side channel flow near the banks, where the stream flow is already slower.

These evaluations can help determine where engineered thermal refuge is likely to be an effective management strategy to mitigate increasingly marginal cold-water fish species conditions in lower New England.

APPENDIX

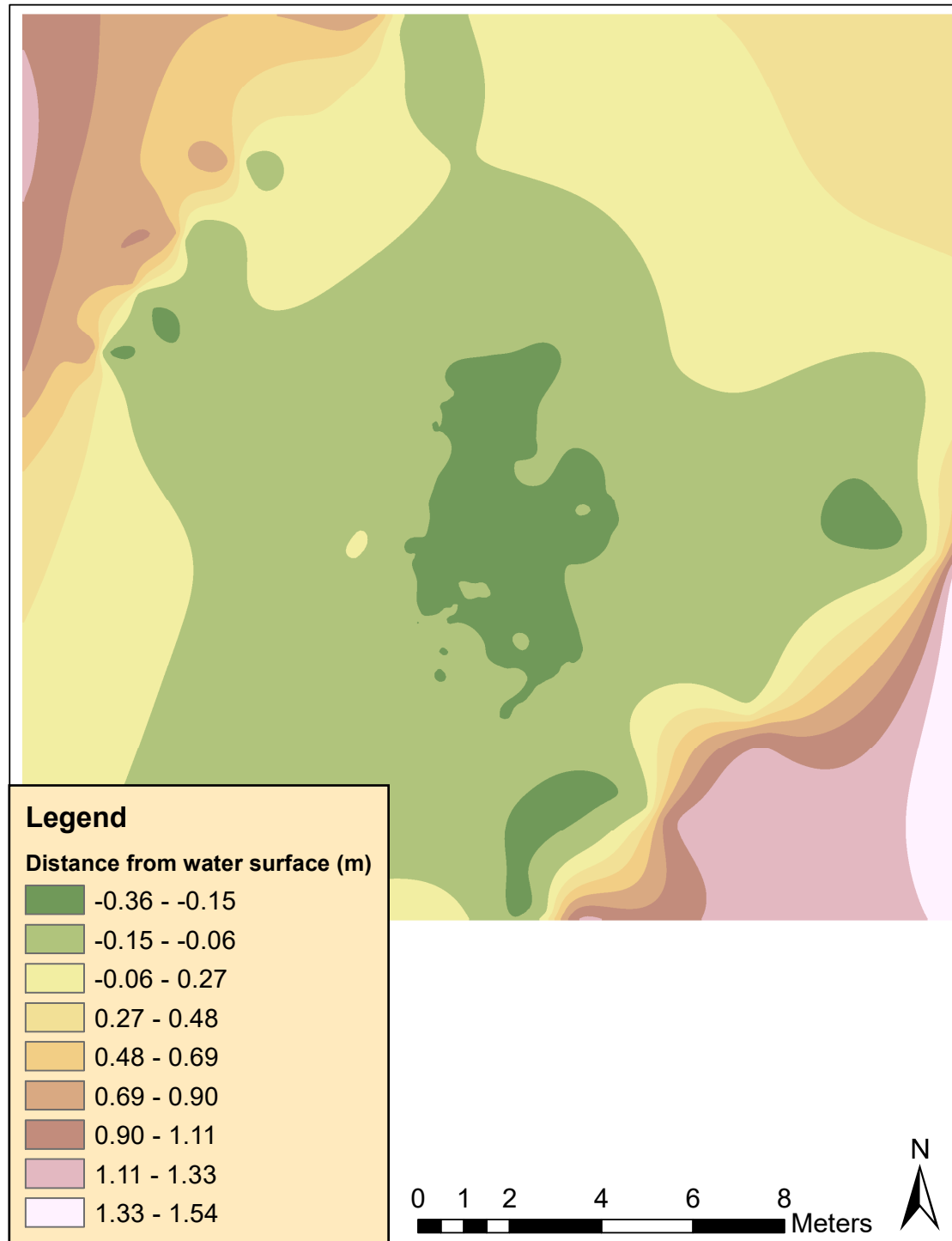


Figure A1. Distance from water surface in meters at the Fenton River field site in 2018 at 1.8 m³/s river discharge.

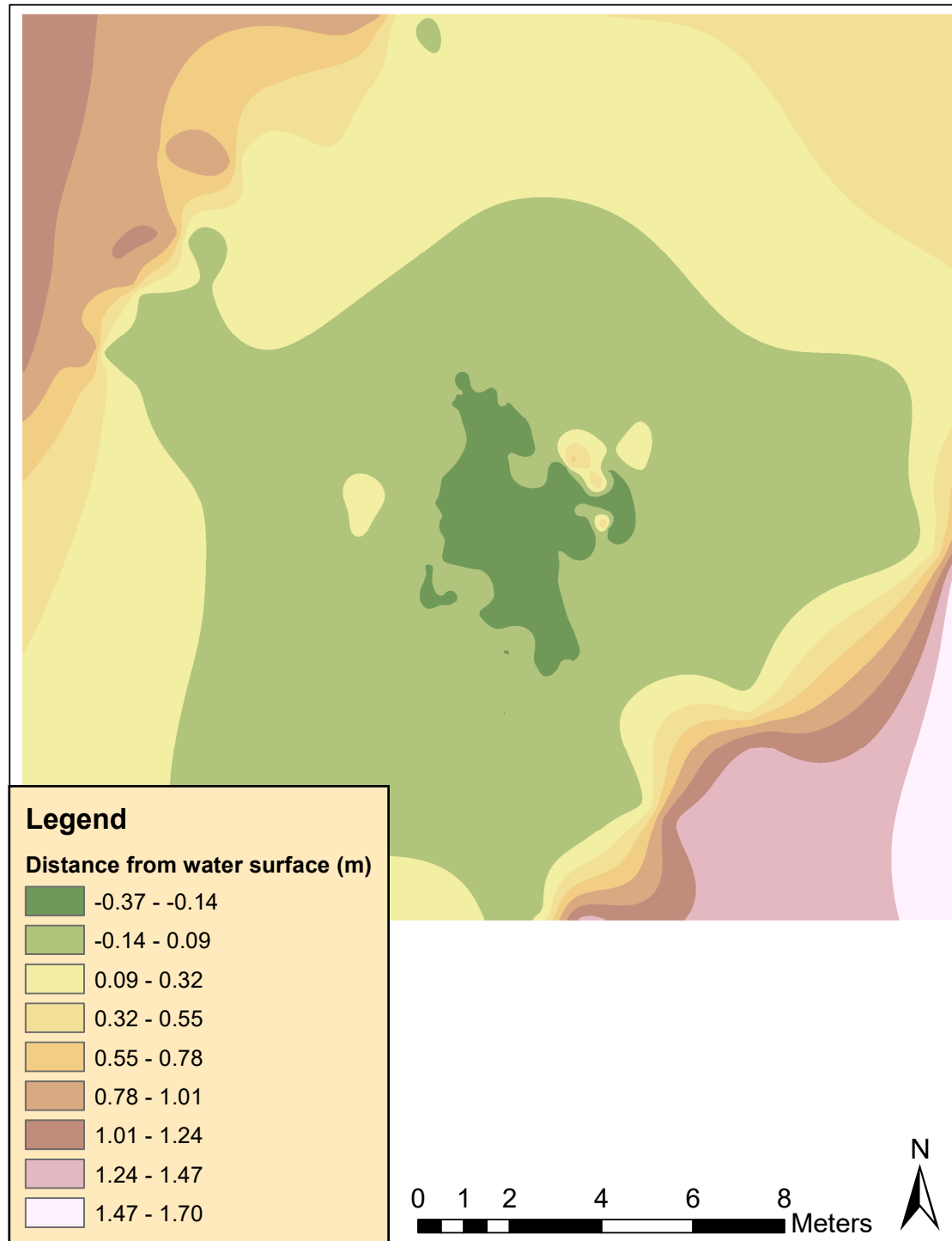


Figure A2. Distance from water surface in meters at the Fenton River field site in 2019 at 0.4 m³/s river discharge.

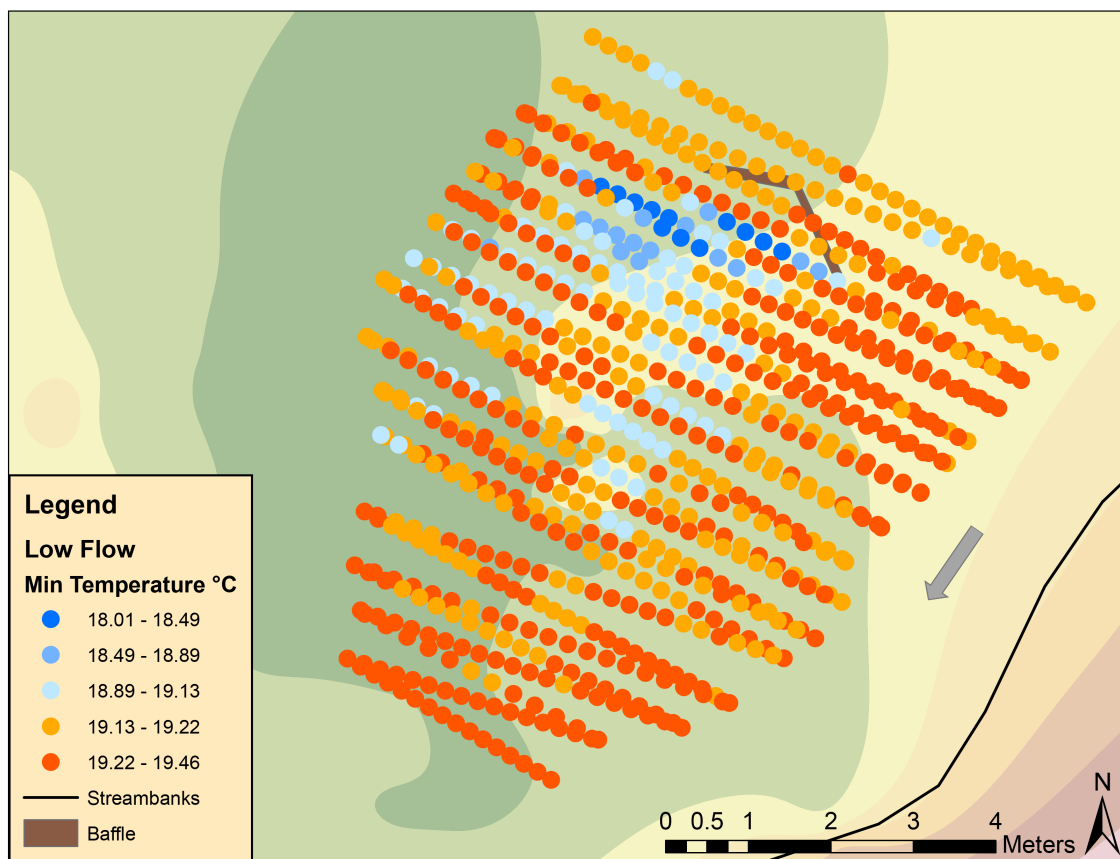


Figure A3. Fiber optic temperature sensing cable data of minimum temperature during low stream discharge ($0.4 \text{ m}^3/\text{s}$), plotted over Fenton river 2019 bathymetry. Arrow indicates flow direction.

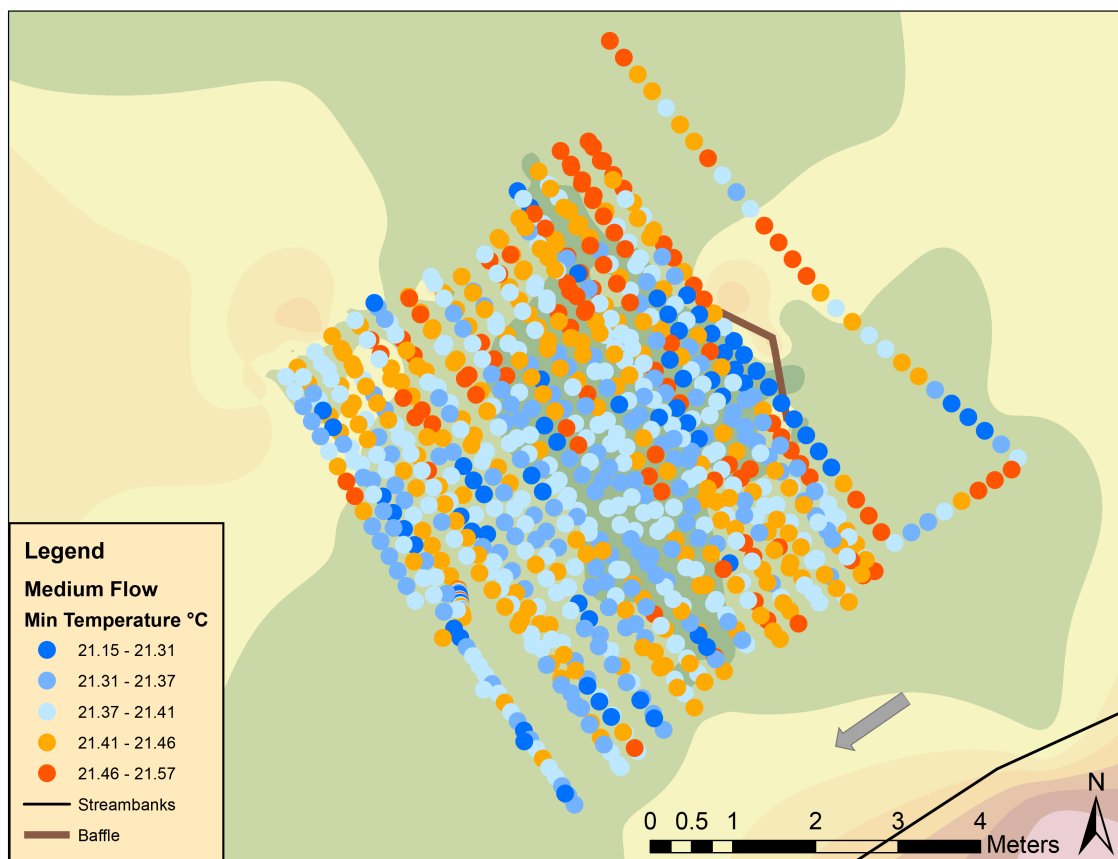


Figure A4. Fiber optic temperature sensing cable data of minimum temperature during medium stream discharge ($1.0 \text{ m}^3/\text{s}$), plotted over Fenton river 2018 bathymetry. Arrow indicates flow direction.

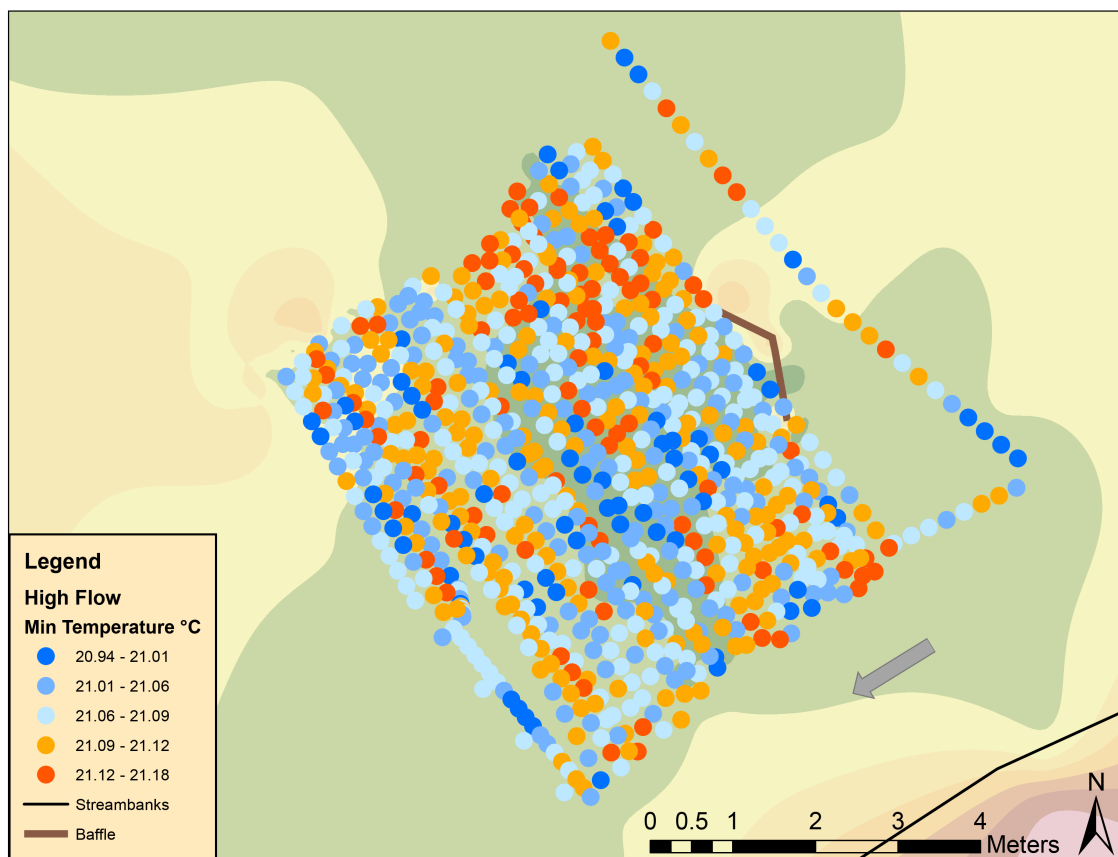


Figure A5. Fiber optic temperature sensing cable data of minimum temperature during high stream discharge ($1.8 \text{ m}^3/\text{s}$), plotted over Fenton river 2018 bathymetry. Arrow indicates flow direction.

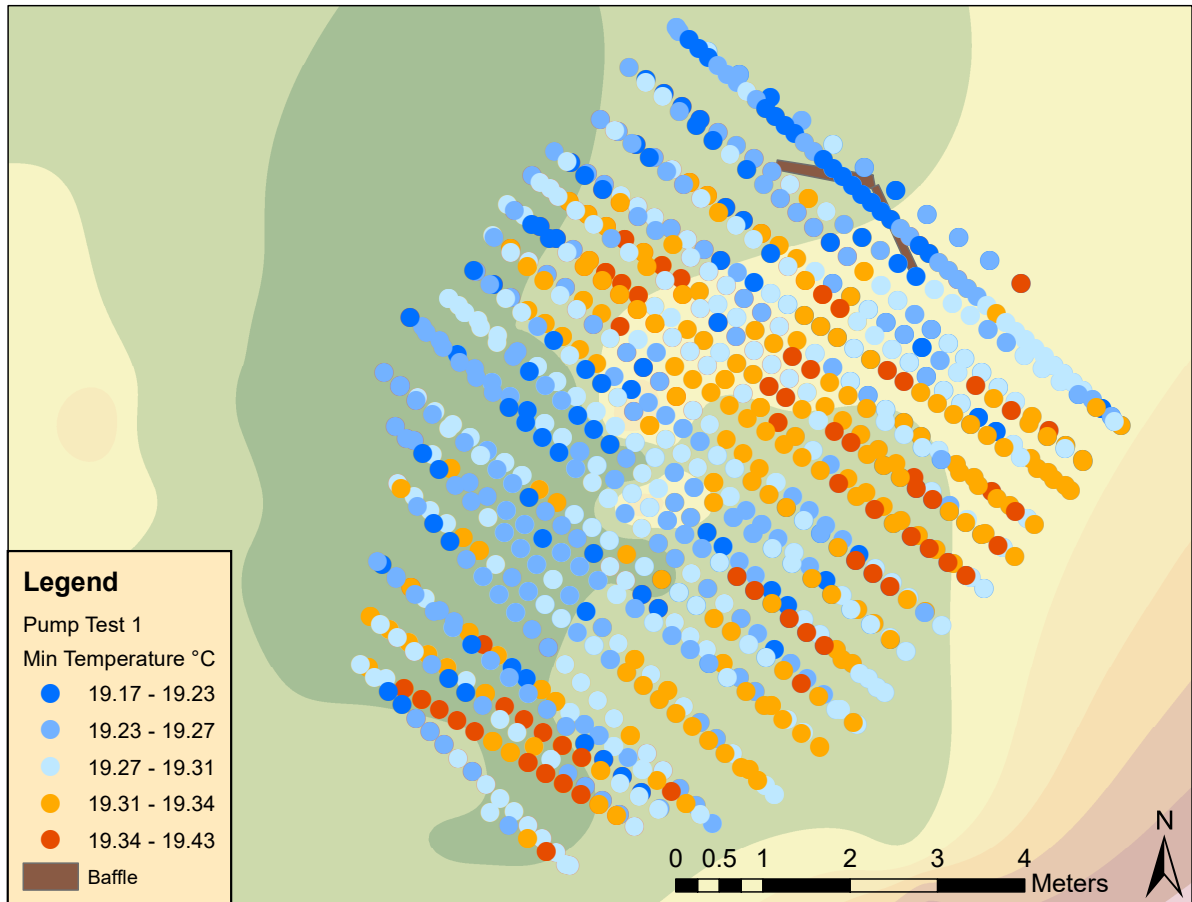


Figure A6. Fiber optic temperature sensing cable data of minimum temperature during pump test 1 (11.4 L/min), plotted over Fenton river 2019 bathymetry.

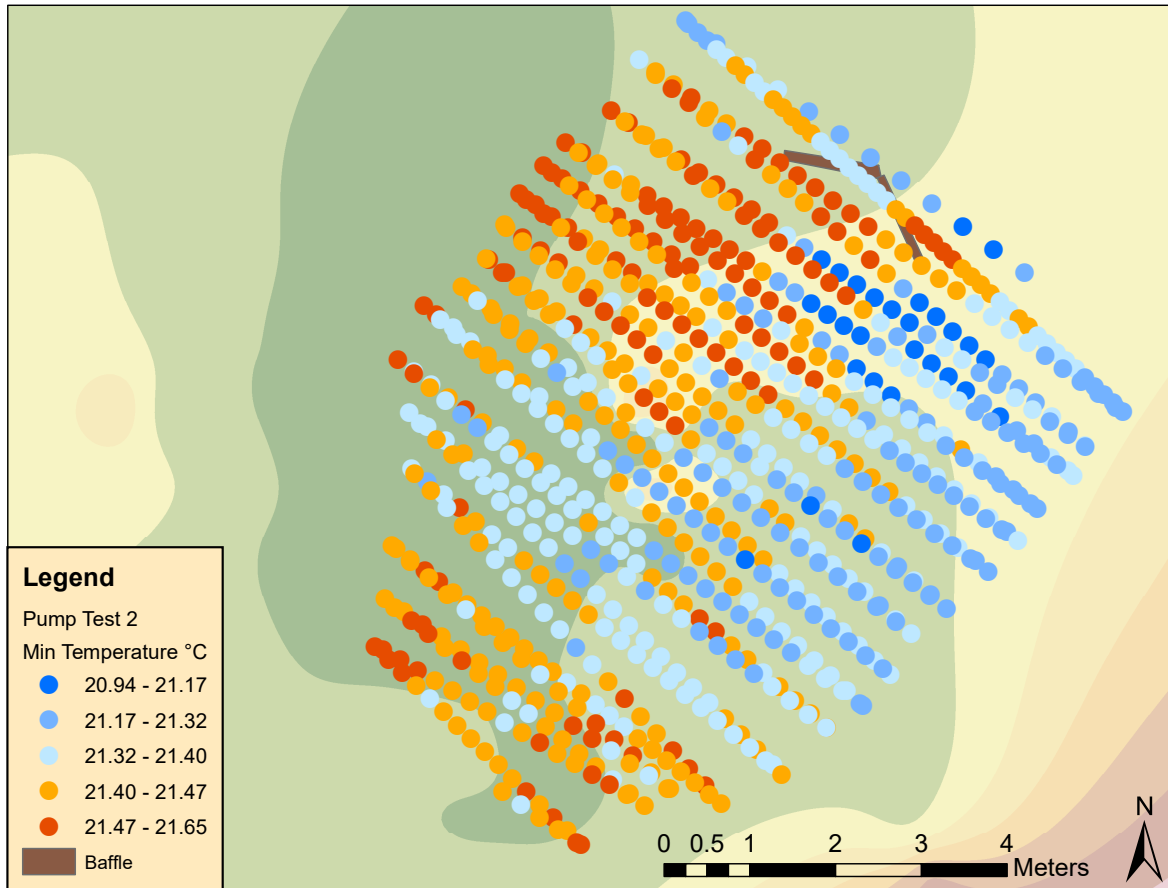


Figure A7. Fiber optic temperature sensing cable data of minimum temperature during pump test 2 (18.9 L/min), plotted over Fenton river 2019 bathymetry.

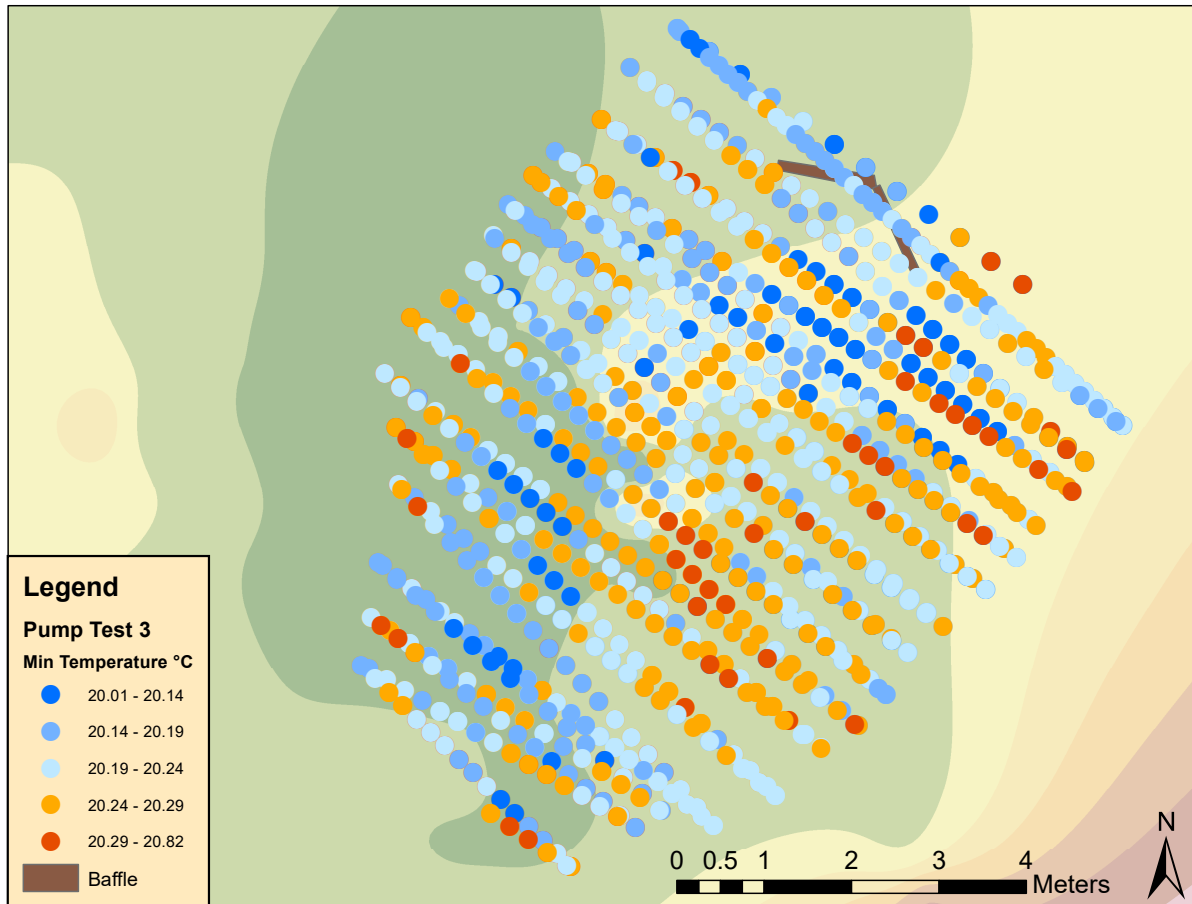


Figure A8. Fiber optic temperature sensing cable data of minimum temperature during pump test 3 (22.7 L/min), plotted over Fenton river 2019 bathymetry.

Works Cited

- Baird, O. E., & Krueger, C. C. (2003). Behavioral Thermoregulation of Brook and Rainbow Trout: Comparison of Summer Habitat Use in an Adirondack River, New York. *Transactions of the American Fisheries Society*, 132(6), 1194–1206.
<https://doi.org/10.1577/T02-127>
- Biron, P. M., Robson, C., Lapointe, M. F., & Gaskin, S. J. (2005). Three-dimensional flow dynamics around deflectors. *River Research and Applications*, 21(9), 961–975.
<https://doi.org/10.1002/rra.852>
- Biron, P. M., Robson, C., Lapointe, M. F., & Gaskin, S. J. (2004). Deflector designs for fish habitat restoration. *Environmental Management*, 33(1), 25–35.
<https://doi.org/10.1007/s00267-003-3080-9>
- Briggs, M., & Hare, D. (2018). Explicit consideration of preferential groundwater discharges as surface water ecosystem control points. *Hydrological Processes*, 32.
<https://doi.org/10.1002/hyp.13178>
- Briggs, M. A., Lane, J. W., Snyder, C. D., White, E. A., Johnson, Z. C., Nelms, D. L., & Hitt, N. P. (2018a). Shallow bedrock limits groundwater seepage-based headwater climate refugia. *Limnologia*, 68, 142-156. <https://doi.org/10.1016/j.limno.2017.02.005>
- Briggs, M. A., Harvey, J. W., Hurley, S. T., Rosenberry, D. O., McCobb, T., Werkema, D., & Lane Jr., J. W. (2018b). Hydrogeochemical controls on brook trout spawning habitats in a coastal stream. *Hydrology and Earth System Sciences*, 22(12), 6383–6398.
<https://doi.org/10.5194/hess-22-6383-2018>
- Briggs, M. A., Johnson, Z. C., Snyder, C. D., Hitt, N. P., Kurylyk, B. L., Lautz, L., ... Lane, J. W. (2018c). Inferring watershed hydraulics and cold-water habitat persistence using

- multi-year air and stream temperature signals. *Science of The Total Environment*, 636, 1117–1127. <https://doi.org/10.1016/j.scitotenv.2018.04.344>
- Briggs, M. A., Lautz, L. K., McKenzie, J. M., Gordon, R. P., & Hare, D. K. (2012). Using high-resolution distributed temperature sensing to quantify spatial and temporal variability in vertical hyporheic flux: HIGH-RESOLUTION HYPORHEIC FLUX PATTERNS. *Water Resources Research*, 48(2). <https://doi.org/10.1029/2011WR011227>
- Chadwick, Joseph G., and Stephen D. McCormick. “Upper Thermal Limits of Growth in Brook Trout and Their Relationship to Stress Physiology.” *The Journal of Experimental Biology*, vol. 220, no. 21, 2017, pp. 3976–3987., doi:10.1242/jeb.161224.
- Champoux, O., Biron, P. M., & Roy, A. G. (2003). The Long-Term Effectiveness of Fish Habitat Restoration Practices: Lawrence Creek, Wisconsin. *Annals of the Association of American Geographers*, 93(1), 42–54. JSTOR.
- Crozier, L.G. and Hutchings, J.A. (2014), Plastic and evolutionary responses to climate change in fish. *Evol Appl*, 7: 68-87.
http://digitalcommons.uconn.edu/ctiwr_specreports/40
- Doll, B., Grabow, G. L., Hall, K. R., Halley, J., Harman, W. A., Jennings, G. D., & Wise, D. E. (2003). *Stream Restoration*. NC State University.
- Domanski, M., Quinn, D., Day-Lewis, F. D., Briggs, M. A., Werkema, D., & Lane, J. W. (2019). DTSGUI: A Python Program to Process and Visualize Fiber-Optic Distributed Temperature Sensing Data. *Groundwater*, n/a(n/a). <https://doi.org/10.1111/gwat.12974>
- Ebersole, J. L., Liss, W. J., & Frissell, C. A. (2003). Cold Water Patches in Warm Streams: Physicochemical Characteristics and the Influence of Shading¹. *JAWRA Journal of the*

American Water Resources Association, 39(2), 355–368. <https://doi.org/10.1111/j.1752-1688.2003.tb04390.x>

Gonia, T. M., Keefer, M. L., Bjornn, T. C., Peery, C. A., Bennett, D. H., & Stuehrenberg, L. C. (2006). Behavioral Thermoregulation and Slowed Migration by Adult Fall Chinook Salmon in Response to High Columbia River Water Temperatures. *Transactions of the American Fisheries Society*, 135(2), 408–419. <https://doi.org/10.1577/T04-113.1>

Handcock, R. N., Torgersen, C. E., Cherkauer, K. A., Gillespie, A. R., Klement, T., Faux, R. N., & Tan, J. (2012). *Thermal infrared remote sensing of water temperature in riverine landscapes*. 85–113.

Hare, D. K., Boutt, D. F., Clement, W. P., Hatch, C. E., Davenport, G., & Hackman, A. (2017). Hydrogeological controls on spatial patterns of groundwater discharge in peatlands. *Hydrology and Earth System Sciences*, 21(12), 6031–6048. <https://doi.org/10.5194/hess-21-6031-2017>

Hitt, Nathaniel P., et al. “Brook Trout Use of Thermal Refugia and Foraging Habitat Influenced by Brown Trout.” *Canadian Journal of Fisheries and Aquatic Sciences*, vol. 74, no. 3, Sept. 2016, pp. 406–18, doi:[10.1139/cjfas-2016-0255](https://doi.org/10.1139/cjfas-2016-0255).

Huntington TG, Richardson AD, McGuire KJ, Hayhoe K. 2009. Climate and hydrological changes in the northeastern United States: recent trends and implications for forested and aquatic ecosystems. *Canadian Journal of Forest Research* 39: 199–212.

Isaak, D. J., Young, M. K., Nagel, D. E., Horan, D. L., & Groce, M. C. (2015). The cold-water climate shield: Delineating refugia for preserving salmonid fishes through the 21st century. *Global Change Biology*, 21(7), 2540–2553. <https://doi.org/10.1111/gcb.12879>

- Kanno, Y., Vokoun, J.C. and Letcher, B.H. (2014), PAIRED STREAM–AIR TEMPERATURE MEASUREMENTS REVEAL FINE-SCALE THERMAL HETEROGENEITY WITHIN HEADWATER BROOK TROUT STREAM NETWORKS. *River Res. Applic.*, 30: 745-755. doi:[10.1002/rra.2677](https://doi.org/10.1002/rra.2677)
- Kløve, B., Ala-Aho, P., Bertrand, G., Gurdak, J. J., Kupfersberger, H., Kværner, J., ... Pulido-Velazquez, M. (2014). Climate change impacts on groundwater and dependent ecosystems. *Journal of Hydrology*, 518, 250–266.
<https://doi.org/10.1016/j.jhydrol.2013.06.037>
- Kurylyk, B. L., MacQuarrie, K. T. B., Linnansaari, T., Cunjak, R. A., & Curry, R. A. (2015). Preserving, augmenting, and creating cold-water thermal refugia in rivers: concepts derived from research on the Miramichi River, New Brunswick (Canada): PRESERVING, AUGMENTING, AND CREATING COLD-WATER THERMAL REFUGIA IN RIVERS. *Ecohydrology*, 8(6), 1095–1108.
<https://doi.org/10.1002/eco.1566>
- Kurylyk, B., Macquarrie, K., & Voss, C. (2014). Climate change impacts on the temperature and magnitude of groundwater discharge from shallow, unconfined aquifers. *Water Resources Research*, 50. <https://doi.org/10.1002/2013WR014588>
- Mathews, K. R., & Berg, N. H. (1997). Rainbow trout responses to water temperature and dissolved oxygen stress in two southern California stream pools. Retrieved June 7, 2019, from Journal of Fish Biology website:
<https://onlinelibrary.wiley.com/doi/abs/10.1111/j.1095-8649.1997.tb01339.x>
- Neill, William H., and John J. Magnuson. “Distributional Ecology and Behavioral Thermoregulation of Fishes in Relation to Heated Effluent from a Power Plant at Lake

- Monona, Wisconsin.” *Transactions of the American Fisheries Society*, vol. 103, no. 4, 1974, pp. 663–710., doi:10.1577/1548-8659(1974)1032.0.co;2.
- Peterson, J.T. and Rabeni, C.F. (1996), Natural Thermal Refugia for Temperate Warmwater Stream Fishes. *North American Journal of Fisheries Management*, 16: 738-746.
doi:[10.1577/1548-8675\(1996\)016<0738:NTRFTW>2.3.CO;2](https://doi.org/10.1577/1548-8675(1996)016<0738:NTRFTW>2.3.CO;2)
- Petty, J. T., Hansbarger, J. L., Huntsman, B. M., & Mazik, P. M. (2012). Brook Trout Movement in Response to Temperature, Flow, and Thermal Refugia within a Complex Appalachian Riverscape. *Transactions of the American Fisheries Society*, 141(4), 1060–1073. <https://doi.org/10.1080/00028487.2012.681102>
- Rosenberry, D. O., Briggs, M. A., Voytek, E. B., & Lane, J. W. (2016). Influence of groundwater on distribution of dwarf wedgemussels (*Alasmodonta heterodon*) in the upper reaches of the Delaware River, northeastern USA. *Hydrology and Earth System Sciences*, 20, 1–17. <https://doi.org/10.5194/hess-20-1-2016>
- Vokoun, J., & Briggs, M. A. (2016, November 17). *Evaluation of created thermal refugia in streams as a climate adaption strategy for fish populations experiencing thermal stress*. University of Connecticut.
- Warner, Glenn S.; Ogden, Fred L.; Bagtzoglou, Amvrossios C.; and Parasiewicz, Piotr, "Long-Term Impact Analysis of the University of Connecticut's Fenton River Water Supply Wells on the Habitat of the Fenton River" (2006). Special Reports. Paper 40.